Dynamic Changes in Lung MicroRNA Profiles During the Development of Pulmonary Hypertension due to Chronic Hypoxia and Monocrotaline

Paola Caruso, Margaret R. MacLean, Raya Khanin, John McClure, Elaine Soon, Mark Southgate, Robert A. MacDonald, Jenny A. Greig, Keith E. Robertson, Rachel Masson, Laura Denby, Yvonne Dempsie, Lu Long, Nicholas W. Morrell and Andrew H. Baker

Arterioscler Thromb Vasc Biol 2010;30;716-723; originally published online Jan 28, 2010;
DOI: 10.1161/ATVBAHA.109.202028
Arteriosclerosis, Thrombosis, and Vascular Biology is published by the American Heart Association. 7272 Greenville Avenue, Dallas, TX 72514
 Print ISSN: 1079-5642. Online ISSN: 1524-4636

Dynamic Changes in Lung MicroRNA Profiles During the Development of Pulmonary Hypertension due to Chronic Hypoxia and Monocrotaline

Paola Caruso, Margaret R. MacLean, Raya Khanin, John McClure, Elaine Soon, Mark Southgate, Robert A. MacDonald, Jenny A. Greig, Keith E. Robertson, Rachel Masson, Laura Denby, Yvonne Dempsie, Lu Long, Nicholas W. Morrell, Andrew H. Baker

Objective—MicroRNAs (miRNAs) are small noncoding RNAs that have the capacity to control protein production through binding "seed" sequences within a target mRNA. Each miRNA is capable of potentially controlling hundreds of genes. The regulation of miRNAs in the lung during the development of pulmonary arterial hypertension (PAH) is unknown.

Methods and Results—We screened lung miRNA profiles in a longitudinal and crossover design during the development of PAH caused by chronic hypoxia or monocrotaline in rats. We identified reduced expression of Dicer, involved in miRNA processing, during the onset of PAH after hypoxia. MiR-22, miR-30, and let-7f were downregulated, whereas miR-322 and miR-451 were upregulated significantly during the development of PAH in both models. Differences were observed between monocrotaline and chronic hypoxia. For example, miR-21 and let-7a were significantly reduced only in monocrotaline-treated rats. MiRNAs that were significantly regulated were validated by quantitative polymerase chain reaction. By using in vitro studies, we demonstrated that hypoxia and growth factors implicated in PAH induced similar changes in miRNA expression. Furthermore, we confirmed miR-21 downregulation in human lung tissue and serum from patients with idiopathic PAH.

Conclusion—Defined miRNAs are regulated during the development of PAH in rats. Therefore, miRNAs may contribute to the pathogenesis of PAH and represent a novel opportunity for therapeutic intervention. **(*Arterioscler Thromb Vasc Biol*. 2010;30:716-723.)**

Key Words: pulmonary hypertension ■ small RNA molecules ■ gene regulation

Pulmonary arterial hypertension (PAH) is a complex disorder characterized by the obstructive remodeling of pulmonary arteries, leading to a progressive elevation in pulmonary arterial pressure (PAP) and subsequent right-sided heart failure and death.[1] Familial PAH is associated in 80% of cases with diverse heterozygous mutations in the gene-encoding bone morphogenetic protein receptor 2 (BMPR-II)[2] and can be associated with mutations in the activin–receptor kinaselike 1 gene.[3] The cause of the variable phenotypic expression of PAH among carriers of mutated *BMPR-II* genes is unclear, and is likely related to environmental and genetic modifiers. Although BMPR-II–related pathways are considered pivotal, many other mediator pathways participate in the pathogenesis of PAH and are being actively investigated, both independently and in combination. For example, the involvement of serotonin in the development of experimental PAH has been recently reported.[4,5] Indeed, important interactions between the serotonin and BMP pathways have recently been described.[6] Rats exposed to hypoxia or injected with the toxin monocrotaline develop pulmonary arterial changes correlated with the development of PAH, including remodeling and elevating PAP.

MicroRNAs (miRNAs) are small noncoding transcripts of 16 to 29 nucleotide RNAs that regulate gene expression posttranscriptionally by targeting mRNAs. Animal miRNAs are processed from longer primary transcripts (primary miRNAs) that can contain multiple miRNAs.[7] This precursor is then processed in 3 steps. First, a complex comprising the nuclear RNase III enzyme Drosha[8] and the double strand (ds) RNA-binding protein Pasha/DGCR8[9] cleaves the primary miRNA in a approximately 60 nucleotides (nt) precursor miRNA hairpin. After this, a shorter precursor is actively transported to the cytoplasm by Exportin-5,[10] where the precursor miRNA undergoes further processing into an approximately 21- to 22-nt duplex (the mature miRNA) by the multidomain ribonuclease Dicer and cofactors.[11] One strand of the duplex is preferentially selected for entry into a silencing complex that includes an argonaute protein. This

Received on: August 12, 2009; final version accepted on: January 13, 2010.

From the Division of Cardiovascular and Medical Sciences, (P.C., J.M., R.A.M., J.A.G., K.E.R., R.M., L.D., and A.H.B.) British Heart Foundation Glasgow Cardiovascular Research Centre, Faculty of Medicine, Glasgow, Scotland; the (M.R.M. and Y.D.) Faculty of Biological and Life Sciences, University of Glasgow, Glasgow, Scotland; the Bioinformatics Core (R.K.), Computational Biology Center, Memorial Sloan Kettering Cancer Center, New York, NY; and the Department of Medicine (E.S., M.S., L.L., and N.W.M.), Addenbrooke's and Papworth Hospitals, University of Cambridge School of Clinical Medicine, Cambridge, England.

Correspondence to Andrew H. Baker, PhD, BSc, Professor of Molecular Medicine, Division of Cardiovascular and Medical Sciences, British Heart Foundation Glasgow Cardiovascular Research Centre, 126 University Ave, University of Glasgow, Glasgow, Scotland. E-mail ab11f@clinmed.gla.ac.uk

Arterioscler Thromb Vasc Biol **is available at http://atvb.ahajournals.org** **DOI: 10.1161/ATVBAHA.109.202028**

mature miRNA guides the argonaute complex to complementary sites on target transcripts.[12]

Recent studies have measured changes in the synthesis of several thousand mRNAs and proteins in response to miRNA transfection or endogenous miRNA knockdown and have found that the major sequence determinant in the miRNA-mediated downregulation of target mRNAs and proteins is the 6-mer "seed" located in the 3′ untranslated terminal regions (UTRs) of mRNAs.[13] Seed sequences in 3′ UTRs were shown to be strongly correlated with reduced protein production, whereas the correlation was weaker but still detectable for seeds in coding sequences.[13] The interaction between miRNA and the seed region leads to a blockade of translation via either cleavage of its mRNA and/or translational repression.

Recently, a substantial level of interest in miRNAs has demonstrated their fundamental role in disease pathogenesis. Many recent studies[14–16] have reported distinct miRNA signatures in cancer cells. In the heart and vasculature, miRNAs are associated with remodeling and the development of hypertrophy and failure.[17–19] In the lung, a recent study[20] has highlighted the regulation of miRNAs after smoke inhalation injury. Herein, we use 2 distinct and commonly used rat models (hypoxic and monocrotaline) of PAH to determine the regulation of miRNAs during disease initiation and progression. We demonstrate time- and insult-dependent changes in miRNA levels that may provide new insights into pathways contributing to the pathobiology of PAH and identify specific miRNAs that are targets for future interventional studies.

Methods

A Supplement (available online at http://atvb.ahajournals.org) provides complete details on the methods used in this study.

Animal Models

Male Sprague-Dawley rats (age, 6 to 7 weeks; weight, 250 to 300 grams) were used throughout. Animals were anesthetized intramuscularly with ketamine, 75 mg/kg, and zylazine, 6 mg/kg; and euthanized at 2, 7, and 21 days after the initiation of hypoxia or after monocrotaline injection. Rats were exsanguinated, and the lungs were removed.

Two-Channel Microarray Experiment

A 2-channel microarray analysis using the MRA-1003 rat miRNA microarray based on miRBase, version 10.1 (LC Sciences, Houston, Tex) was used. Supplemental Figure IA depicts the design of the miRNA microarray study investigating PAH in rats. To assess the statistical significance of intergroup differences, rank products[21] were used. Significance was assessed using the false discovery rate multiple testing correction method,[22] with a false discovery rate cutoff of 5%.

Prediction of Potential miRNAs Targets

A list of targets for miR-21, miR-22, miR-30c, miR-451, and miR-322 was obtained by searching 3′ UTR sequences of rat mRNAs for the seeds of miRNAs. Rat mRNAs were downloaded from the USCS Genome Browser (available online at http://genome.ucsc.edu/). Target mRNA expression was assessed in the same samples used for miRNA analysis using assay kits (TaqMan, Applied Biosystems, Foster City, Calif).

Transforming Growth Factor β_1 and BMP4 Rat Pulmonary Artery Endothelial Cells Stimulation

Passage 4 rat pulmonary artery endothelial cells (PASMC) were cultured in 6-well plates in growth media. After 24 hours, the media was replaced with serum-free media and cells were incubated for a further 24 hours. Wells were then incubated with 1 ng/mL of transforming growth factor (TGF) β_1 or 10 ng/mL of BMP4 or with Dulbecco-modified Eagle growth media containing 0.1% heat-inactivated fetal calf serum as a negative control. Total RNA was extracted after 5 and 24 hours of stimulation and stored for quantitative polymerase chain reaction (q-PCR) analysis of miR-451, miR-21, miR-22, miR-30c, and let-7f expression.

Results

Time Course of Pulmonary Hemodynamics in Hypoxia-Exposed and Monocrotaline-Treated Rats

Hemodynamic studies confirmed that both chronic hypoxia and monocrotaline exposure resulted in the development of PAH. In control rats, the mean PAP was 20.0±0.8 mm Hg. In hypoxic animals, the mean PAP after 2, 7, and 21 days was 24.8±1.2, 33.9±1.1, and 40.7±1.9 mm Hg, respectively. In monocrotaline-exposed animals at the same time points, the mean PAP was 19.9±0.8, 19.3±1.4, and 29.6±2.1 mm Hg, respectively.

Analysis of Genes Critical for miRNA Biogenesis After the Initiation of PAH

First, we assessed the mRNA levels for genes critical to miRNA biogenesis (ie, Dicer, Drosha, Pasha/DGCR8, and Exportin-5) by TaqMan q-PCR analysis. Interestingly, we observed that in vivo exposure to hypoxia induced a marked and sustained decrease in mRNA for Dicer (Figure 1A and Supplemental Figure IIA). Monocrotaline injury had a significant effect on Dicer expression only 21 days after the treatment (Figure 1A). We also quantified Dicer, Drosha, Pasha/DGCR8, and Exportin-5 mRNA expression in 24-hour hypoxic rat pulmonary artery fibroblasts (PAF), extracting RNA in sextuplicate from cells. In vitro, Dicer expression was significantly downregulated by hypoxia (Figure 1B and Supplemental Figure IIB).

Global miRNA Profiling of the Lungs of Hypoxia- and Monocrotaline-Treated Rats

The expression level of 350 miRNAs in the lung was investigated using a 2-channel microarray experiment, allowing us to identify their expression pattern during the first stages of PAH pathogenesis (Supplemental Figure IB and Supplemental Table I). We confirmed the prominent expression of miR-195 and miR-200c in rat lung samples of control animals (data not shown), consistent with the previous identification of these miRNAs as the only lung-specific miRNAs.[23] The expression of miR-322, miR-451, miR-21, miR-22, miR-30c, let-7f, and let-7a was the most significantly altered (Supplemental Table II) and was, therefore, selected for further analysis. Further visualization of miRNA dysregulation was observed using dot plots for average values in each group plotted against each condition and time point (Figure 2).

Validation of the miRNA Dysregulation

To validate the microarray analysis, the expression level of miR-322, miR-451, miR-21, miR-22, miR-30c, let-7f, and let-7a plus a control miRNA that was not altered in the lungs of treated animals compared with controls (miR-145) was analyzed by TaqMan q-PCR using total RNA extracted from both hypoxic and monocrotaline-treated rats. As expected, and in agreement with the profiling data, miR-145 levels were not altered under either condition (Figure 3 and Supplemental Figure III). In

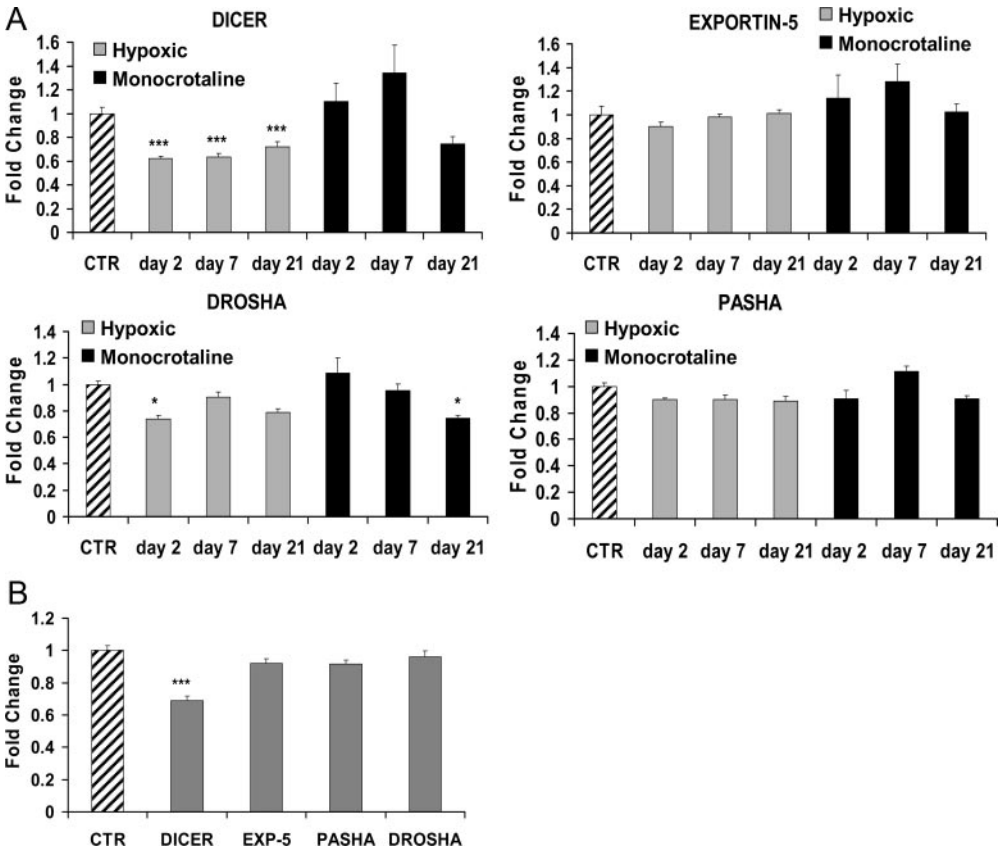

Figure 1. In vivo and in vitro expression level of Dicer, Exportin-5, Drosha, and Pasha in hypoxic and monocrotaline-treated rats. A, q-PCR analysis of hypoxic and monocrotaline-injected rats after 2, 7, and 21 days of exposure. Total RNA was extracted from hypoxic (gray bars) or monocrotaline-injected (black bars) male rats at the age of 6 weeks. Results were normalized to GAPDH values and expressed as relative fold change, with an arbitrary value of 1 assigned to the control (CTR) group. For statistical analysis, we conducted a *t* test, checking each hypoxic or monocrotaline group vs the CTR group (*$P<0.05$ and ***$P<0.001$ vs CTR samples). B, q-PCR analysis of hypoxic rat pulmonary arterial fibroblasts (PAF) showing the expression level of Dicer, Exportin-5 (Exp5), Pasha, and Drosha after 24 hours of exposure. This experiment was performed with total RNA extracted from both the CTR and the hypoxic cells. Results were normalized to GAPDH values (***$P<0.001$ vs CTR samples).

contrast, miR-451, miR-322, let-7f, let-7a, miR-21, miR-22, and miR-30c were significantly altered after injury (Figure 3 and Supplemental Figure III). In particular, miR-451 expression showed a strong upregulation in the hypoxic samples, and reached a maximum 7 days after monocrotaline injection. MiR-322 was significantly upregulated just 7 days after the injury for both the models before returning to control levels by day 21. MiR-22 expression showed differences between the 2 models, resulting in maximal downregulation after 21 days in hypoxic conditions and 2 days after a monocrotaline injection. MiR-21 and miR-30c showed a significant downregulation in the monocrotaline and in the hypoxic model alone, respectively (Figure 3 and Supplemental Figure III). Let-7f expression was downregulated in both the models at early time points in the hypoxic model (2 and 7 days after the induction of hypoxia) and at later time points in the monocrotaline model (21 days after the injection), whereas let-7a showed a significant downregulation only 21 days after monocrotaline injection (Figure 3 and Supplemental Figure III). We also quantified the expression level of the miR-17–miR-92a cluster (miR-17, miR-19b, miR-20a, and miR-92) in consideration of its recent involvement in the regulation of BMPR-II. An array analysis showed no significant dysregulation (Supplemental Table III). MiR-18a and miR-19a were not assessed because they showed low expression on the array. TaqMan q-PCR validations showed a small, but significant, upregulation of miR-17, miR-19b, miR-20a, and miR-92 in the samples (Supplemental Figure IV), consistent with a recent study.[24]

In Vitro Validation of miRNA Expression Level

Next, we assessed the expression level of miRNAs that were downregulated (miR-22, miR-21, miR-30c, and let-7f) in in vitro models of hypoxic injury to determine whether the hypoxic insult in vitro paralleled the effect of miRNA profiles in vivo. We extracted total RNA from normoxic and 24-hour hypoxic rat PAFs and rat PASMCs and analyzed the samples by TaqMan q-PCR for miRNA levels, normalizing this to the internal control U87. The expression pattern for miR-22, miR-21, let-7f, and miR-30c was quite similar to the in vivo analysis. In PAFs, miR-22, let-7f, and miR-30c were significantly downregulated, whereas miR-21 showed a similar expression level in both normoxic and hypoxic cells (Figure 4A). In PASMCs, both miR-22 and miR-30c showed a significant downregulation, whereas miR-21 and let-7f did not show altered expression after hypoxic treatment (Figure 4B). Thus, the exposure of rat PAFs and PASMCs in vitro to hypoxia correlated well with the changes in miRNAs observed in vivo. We also used 2 in vitro

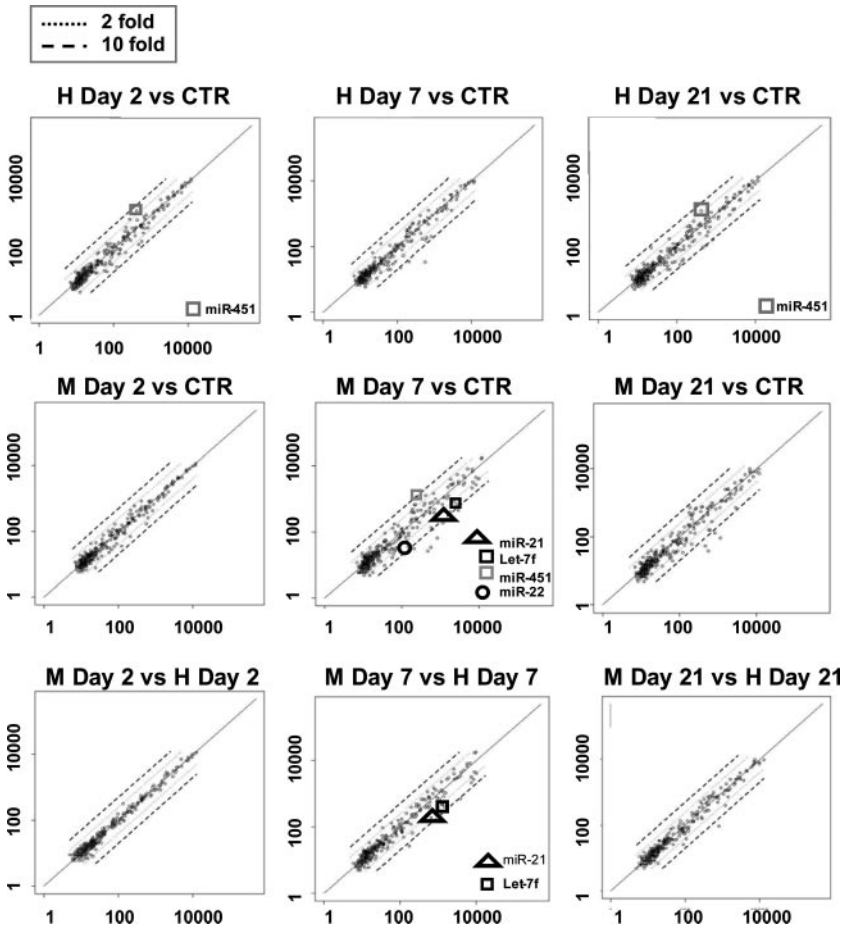

Figure 2. Modulation of miRNA dysregulation in PAH. Global miRNA data sets were plotted on a log scale against each other to identify those miRNAs that are dysregulated both within disease groups and compared with controls and longitudinally. Lines representing 2.5- and 5.0-fold changes are shown. In each case, the x- and y-axes represent the average of 5 per group.

human cell models for assessing miRNA modulation. We analyzed human fetal PAFs and human pulmonary artery endothelial cells (PAEC) after 24-hour exposure to hypoxia. The analysis of PAFs showed a significant dysregulation of all 4 miRNAs; in hypoxic PAECs, only miR-30c was modestly downregulated (Supplemental Figure V). Because TGF-β and BMP are important regulators of pulmonary vascular SMC signaling in PAH[25] and the miR-451 promoter contains an Smad-responsive element,[26] we exposed rat PASMCs to TGF-β_1 and BMP4 and assessed miR-451 levels. Both agonists induced miR-451 levels significantly after 5 hours of stimulation (Figure 4C). Notably, values returned to the unstimulated level by 24 hours (Figure 4C). For a better understanding of the role of TGF-β_1 in the dysregulation of our miRNAs of interest, we also quantified the expression level of miR-21, miR-30, miR-22, and let-7f after stimulation. TGF-β_1 stimulation induced the same kind of dysregulation we observed in hypoxic and monocrotaline-treated rats. In fact, all 4 miRNAs (miR-21, miR-22, miR-30c, and let-7f) were downregulated in a time-dependent manner (Figure 4D).

Prediction of Potential miRNA Targets

To identify a list of mRNA targets for miR-21, miR-22, and miR-30c, we screened the 3′ UTRs of mRNAs for the 6-mer seeds of the miRNAs of interest. The seed is Watson-Crick consecutive base pairing between mRNAs and the miRNAs at nucleotide positions 2 to 7 from its 5′ end. It has been demonstrated using an unbiased computational approach applied to high-throughput pulsed SILAC data sets that the seed sequence in the 3′ UTR is a primary motif that correlates with both mRNA degradation and translational repression.[13] Seed-based target prediction methods had the highest overlap with pulsed SILAC data. The accuracy of target prediction methods is improved by using evolutionary conservation as an additional filter (PicTar, TargetScanS, or Diana). However, the false-positive rate of these target prediction methods, even with conserved seed incorporation, is still around 40%. The relatively mild extent of miRNA-mediated target downregulation has been found to depend on the number of seeds of the miRNA of interest and the distance between the adjacent seeds. Multiple nonconserved seeds, in particular those located at optimal distances of less than 40 nt, act synergistically.[13,27] For example, 2 nonconserved seeds located within 40 nt appear to exert the same effect as a single conserved seed (Raya Khanin, PhD, unpublished data, 2009). In addition, seeds for different miRNAs within an optimal distance may cooperatively regulate 1 target.[27] The current target prediction algorithms do not consider this. Therefore, we opted to search for 6-mer seeds for miRNAs of interest in 3′ UTRs of rat mRNAs. In particular, we focused on those proteins that have multiple seeds for 1 or more miRNAs located within a small distance on 3′ UTR. Based on this, we generated a number of targets for downregulated miRNAs (miR-21, miR-30c, and miR-22) (Supplemental Table IV). The same strategy has been used for preliminary identifi-

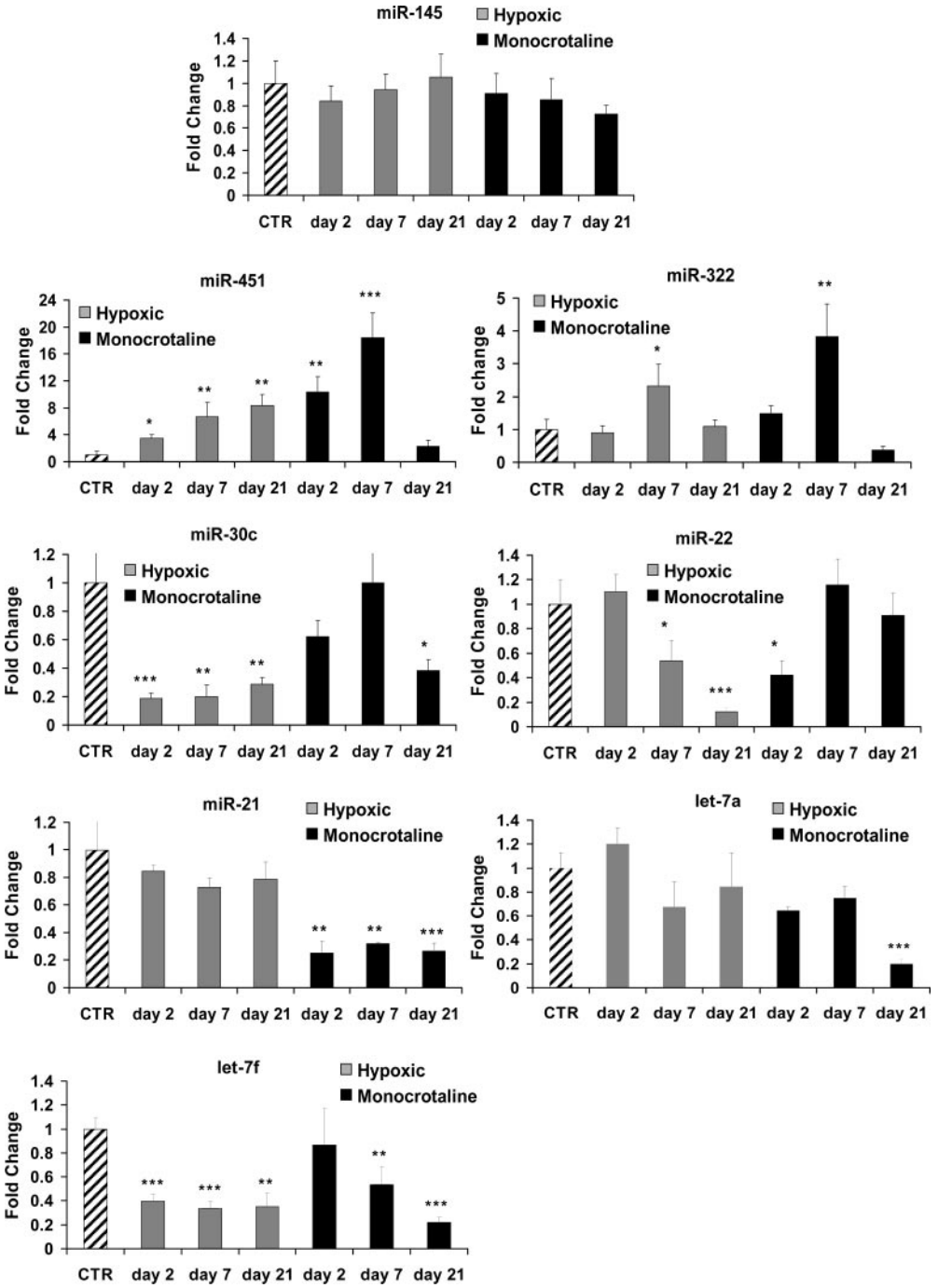

Figure 3. Validation of miRNA dysregulation. q-PCR analysis of hypoxic and monocrotaline-injected rats after 2, 7, and 21 days of exposure. Total RNA was extracted from hypoxic (gray bars) or monocrotaline-injected (black bars) male rats at the age of 6 weeks. Results were normalized to U87 values and expressed as relative fold change, with an arbitrary value of 1 assigned to the control (CTR) group. $^{*}P<0.05$, $^{**}P<0.005$, and $^{***}P<0.001$ vs CTR samples.

cation of the potential targets of the 2 upregulated miRNAs (miR-451 and miR-322) (Supplemental Table V). Several targets identified for the upregulated miRNA group are in common with the group of downregulated miRNAs.

Analysis of miR-21, miR-22, and miR-30c Targets in Hypoxic and Monocrotaline-Treated Lungs

Based on the targets identified in the Supplemental Table IV, we performed TaqMan q-PCR validation analysis on the same sample sets used for miRNA profiling (Supplemental Figure VI). In general, a number of the predicted genes, but not all, were regulated as expected. For example, KCNJ6 mRNA levels were significantly enhanced after both hypoxia- and monocrotaline-induced injuries (Supplemental Figure VI). MiR-21 was only downregulated in monocrotaline-induced injury. Likewise, TACC1, which has predicted targets for miR-21 and miR-30c, was only upregulated in the monocrotaline-treated lungs, suggesting that miR-21 is a key regulator in monocrotaline-induced

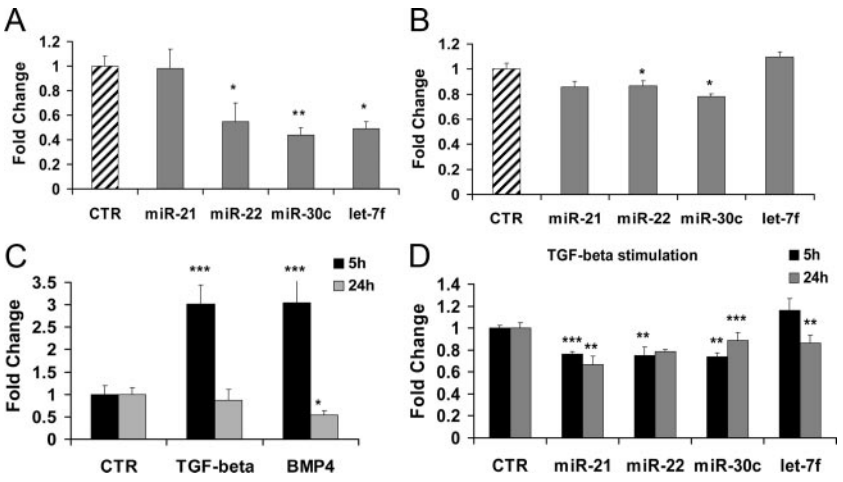

Figure 4. miRNA expression is regulated by hypoxia in vitro and TGF-β_1–BMP4 stimulation can induce the significant dysregulation of miR-451, miR-21, miR-22, miR-30c, and let-7f in PASMCs. A and B, q-PCR analysis of hypoxic rat pulmonary arterial fibroblasts (PAFs) (A) and PASMCs (B) showing the expression level of miR-21, miR-22, miR-30c, and let-7f after 24 hours of stimulation. These experiments were performed with total RNA extracted from both the control (CTR) and the hypoxic cells. Results were normalized to U87 values and expressed as relative fold change, with an arbitrary value of 1 assigned to the CTR group. C and D, TGF-β_1 and BMP4 stimulation of rat PASMCs. Passage 4 primary cells were stimulated with total RNA extracted after 5 and 24 hours of stimulation from both non-treated and stimulated rat PASMCs, and each sample was analyzed in q-PCR triplicate for testing miR-451 (C) and miR-21, miR-22, miR-30c, and let-7f (D) expression level after 5 and 24 hours of stimulation. Results were normalized to U87 values and expressed as relative fold change, with an arbitrary value of 1 assigned to the CTR group. *$P<0.05$, **$P<0.005$, and ***$P<0.001$ vs CTR samples.

PAH. Protein phosphatase 2, regulatory subunit B′, epsilon isoform (PPP2R5E) was upregulated only after monocrotaline-induced injury, again perhaps indicative of miR-21 regulation. Similarly, transforming growth factor, beta receptor 1 (TGFBR1), a target of miR-22, showed significant upregulation selectively in the monocrotaline model. The upregulation of YWHAZ and TNRC6A only in the monocrotaline-treated rats could be indicative of a significant role of miR-30c in gene regulation after injury (Supplemental Figure VI). To validate the up-regulation of targets at the protein level, we quantified by western blot analysis the expression level of TGFBR1 in monocrotaline day 7-treated and untreated rats. The signal obtained from 4 samples for each group showed a significant upregulation in monocrotaline-treated rats (Figure 5A). We selected this target again for the relevant role of TGF-β_1 in pulmonary vascular SMC signaling in PAH. On day 7, we also localized TGFBR1 protein in paraffin sections from control and monocrotaline-treated rat lungs with immunohistochemistry assays. Again, this experiment showed TGFBR1 upregulation in the monocrotaline model 7 days after the treatment (Figure 5B–D).

Expression Level of miR-21 and miR-451 in Samples From Idiopathic Pulmonary Arterial Hypertension in Humans

Considering the high level of dysregulation both in vivo and in vitro of miR-451 and miR-21, and TGF-β_1 effect on their expression level, we analyzed total RNA extracted from paraffin-embedded lungs of patients with idiopathic pulmonary arterial hypertension (PAH) and unaffected controls. A significant downregulation of miR-21 was observed (Figure 6A). Similarly, miR-21 downregulation in human samples was also demonstrated in serum samples obtained from patients with idiopathic PAH when compared with serum obtained from unaffected controls (Figure 6B). MiR-451 was unaltered in both lung tissue and serum (Figure 6).

Discussion

Gene regulation by miRNA in the progression of several diseases is becoming increasingly relevant. Herein, we profiled miRNA signatures in the rat lung and compared them longitudinally with rats exposed to either chronic hypoxia or monocrotaline injuries at 2, 7, and 21 days. We show that a small subset of miRNAs is significantly changed (eg, miR-21, miR-22, miR-30c, let-7f, let-7a, miR-322, and miR-451). These miRNA profiles were validated by TaqMan q-PCR. The regulation of these miRNAs was also mimicked in in vitro models involving exposure of rat PAFs, rat PASMCs, human PAFs, and human PAECs to hypoxia, or exposure of rat PASMCs to TGF-β or BMPs. By using bioinformatics analysis, we also predicted the

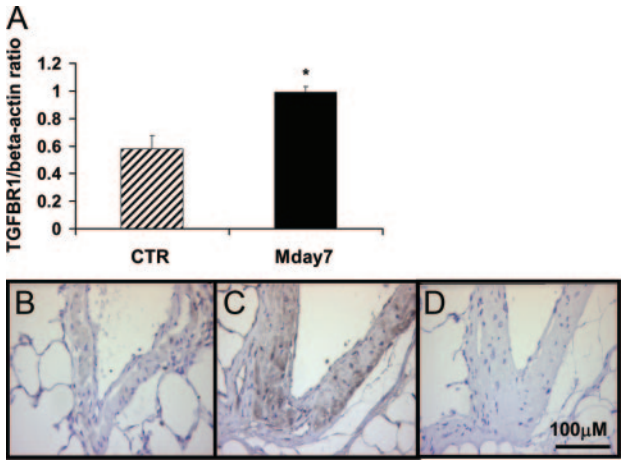

Figure 5. Assessment of TGFBR1 protein expression level in total rat lung protein extracts and its localization in rat lung paraffin sections. A, TGFBR1 expression level was quantified by Western blot analysis in proteins extracted from lung samples of monocrotaline-treated rats on day 7 (Mday7) and control (CTR) rats. Four samples were tested for each group, and the intensity of the Western blot bands was measured using specific software (Scion Image software). The resulting quantification bars are represented in the graph, with the monocrotaline day 7 group represented by the gray bar (*$P<0.05$ vs CTR samples). TGFBR1 was localized in lung paraffin sections using an immunohistochemistry assay. B, TGFBR1 staining in CTR rat lungs. C, TGFBR1 staining in lungs after monocrotaline exposure for 7 days. D, Lung stained with a nonimmune isotype-IgG CTR antibody.

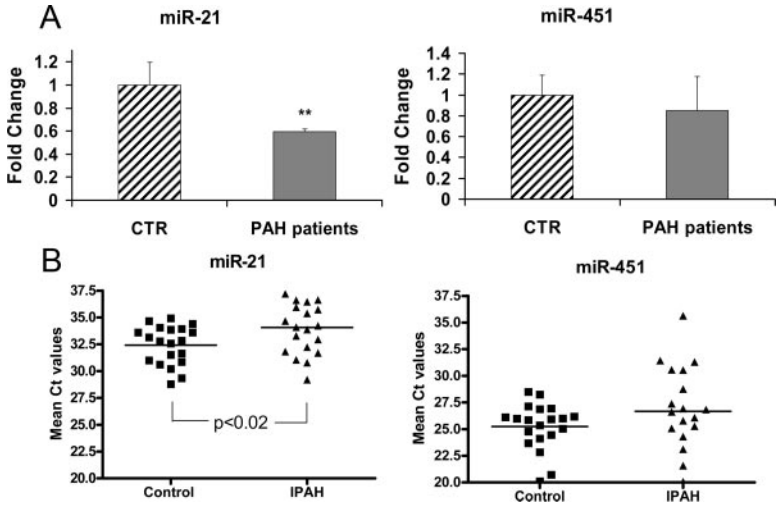

Figure 6. miR-21 and miR-451 expression level in idiopathic PAH human samples. A, q-PCR analysis of miR-21 and miR-451 expression level in paraffin-embedded human lungs of patients with idiopathic PAH and controls (CTRs). Samples were normalized to Rnu-48 values and expressed as relative fold change, with an arbitrary value of 1 assigned to the CTR group (**$P<0.005$ vs CTR samples). B, q-PCR analysis showing Ct values for miR-21 and miR-451 expression in serum taken from patients with idiopathic PAH (IPAH) and unaffected CTRs. Ct, Cycle threshold, the number of cycles it takes for a sample to reach the level where the rate of amplification is the greatest during the exponential phase.

target sequences for these miRNAs, which predicted relevance to genes involved in pathways known to be critical in PAH and potentially novel genes. A number of predicted targets were regulated in a manner predicted by the miRNA dysregulation pattern. Moreover, an analysis of targets of the downregulated miRNAs (ie, miR-21, miR-22, and miR-30c) and targets of the upregulated miRNAs (ie, miR-451 and miR-322) showed the presence of several target proteins in common, an indication of the potential complex regulation of such targets in vivo. This could explain why the expression level of several targets did not always correlate with miRNA modulation.

Hypoxia and monocrotaline induced consistent changes in miR-451 and to some extent miR-30c, yet regulated miR-21 and miR-22 differently. This suggests that hypoxia- and monocrotaline-induced PAH share some common elements relating to miRNA regulation and differential regulation. Such differential regulation is not entirely unexpected as the result of the differential pathobiology induced by hypoxia and monocrotaline. Monocrotaline challenge mainly targets the pulmonary vascular endothelium and triggers the inflammatory process, especially monocyte recruitment, both of which play an important role in the course of human PAH.[28–30] The course of development of PAH is also different in each model, as is well-known and confirmed in the present study. Hypoxia stimulates changes in medial, adventitial, and endothelial layers of the pulmonary artery; however, hypoxia leads to less inflammation than monocrotaline. The underlying pathobiology in both models leads to differences at the protein level. For example, by using a proteomic approach, it has recently been shown that in the hypoxic model, proteins of the nitric oxide, carbon monoxide, and vascular endothelial growth factor pathways are significantly increased.[31] In the monocrotaline model, proteins involved in serotonin synthesis, the enhanced unfolded protein response, and intracellular chloride channels are significantly elevated.[31]

Dysregulation of BMP and TGF-β signaling occurs in both the hypoxic and monocrotaline models of PAH. Specifically, reduced lung expression of BMPR-II and reduced signaling via the downstream Smad1/5 pathway are observed.[25] Conversely, increased TGF-β signaling is observed, with increased Smad3 phosphorylation and increased expression of TGF-β target genes.[25] These effects are greater in the monocrotaline model compared to exposure to chronic hypoxia. Interestingly, the promoter region of miR-451 possesses an Smad3 response element.[26] Thus, activation of TGF-β signaling could be responsible for the increased expression of miR-451 observed in our studies. TGF-β stimulation was able to induce the downregulation of miR-21, miR-22, miR-30c, and let-7f in our experiments.

The involvement and importance of miR-21 in disease pathogenesis is becoming increasing well documented, especially for the cardiovascular system. In blood vessel remodeling after acute vascular injury, miR-21 is rapidly upregulated when it associated with the development of intimal hyperplasia.[32] Knockdown of miR-21 blocked development of the lesion, suggesting a critical role for miR-21 in vascular pathology. Herein, we show that miR-21 is selectively and consistently (at all 3 points) downregulated after monocrotaline injection, but not during hypoxic exposure. Therefore, in the lung after exposure to monocrotaline, but not hypoxia, vascular remodeling is associated with a substantial loss of miR-21. Therefore, it will be important in future studies to ascertain the role of miR-21 in monocrotaline-induced pathology. BMPs are known to drive smooth muscle cell differentiation via upregulation of miR-21.[33] The downregulation of miR-21 in the monocrotaline model, possibly related to reduced BMP signaling,[25] may be involved in the alteration of the smooth muscle cell phenotype that is seen in PAH. Similarly, for other modulated miRNAs, it will be critical to ascertain their role in disease pathology and to define the potential effect of miRNA modulation in disease prevention. In the future, it will be important to generate reliable methods to deliver miRNA therapeutics to the lung efficiently and selectively. This might require new strategies to modulate the tropism of a gene delivery system (eg, viruses) and to generate selective agents and cells.

We have focused on those miRNAs showing the largest changes after the onset of injury. Three important recent studies have shown that even subtle changes in miRNA lead to large changes in phenotypes.[13,27,34] Thus, the large changes we have observed in miRNAs in this study are likely to strongly affect the cell biology and pathobiology associated with the development of PAH. The downregulation of miR-21 in idiopathic PAH human samples suggests a potential important role for this

miRNA in human PAH. On the contrary, we did not observe miR-451 upregulation in the same samples.

In summary, for the first time to our knowledge, we have reported the global miRNA profiles of rat lungs after exposure to hypoxia and monocrotaline injury. This highlights the potential importance of miRNA in disease progression and possible targets (either the miRNAs themselves or their mRNA targets) for future therapeutic intervention.

Acknowledgments

We thank Nicola Britton, BS, and Gregor Aitchison, BS, for their technical assistance and the Cambridge NIHR Biomedical Research Centre for its support.

Sources of Funding

This study was supported by the British Heart Foundation and the Biological and Biotechnology Research Council of England.

Disclosures

None.

References

1. Rich S, Dantzker D, Ayres S, Bergofsky E, Brundage B, Detre K, Fishman A, Goldring R, Groves B, Koerner S. Primary pulmonary hypertension: a national prospective study. *Ann Intern Med*. 1987;107: 216–223.
2. International PPH Consortium; Lane KB, Machado RD, Pauciulo MW, Thomson JR, Phillips JA 3rd, Loyd JE, Nichols WC, Trembath RC. Heterozygous germline mutations in BMPR2, encoding a TGF-β receptor, cause familial primary pulmonary hypertension. *Nat Genet*. 2000;26:81–84.
3. Harrison RE, Flanagan JA, Sankelo M, Abdalla SA, Rowell J, Machado RD, Elliott CG, Robbins IM, Olschewski H, McLaughlin V, Gruenig E, Kermeen F, Halme M, Räisänen-Sokolowski A, Laitinen T, Morrell NW, Trembath RC. Molecular and functional analysis identifies ALK-1 as the predominant cause of pulmonary hypertension related to hereditary haemorrhagic telangiectasia. *J Med Genet*. 2003;40:865–871.
4. Dempsie Y, Morecroft I, Welsh D, MacRitchie N, Herold N, Loughlin L, Nilsen M, Peacock A, Harmar A, Bader M, MacLean M. Converging evidence in support of the serotonin hypothesis of dexfenfluramine-induced pulmonary hypertension with novel transgenic mice. *Circulation*. 2008;117:2928–2937.
5. Lawrie A, Spiekerkoetter E, Martinez E, Ambartsumian N, Sheward W, MacLean M, Harmar A, Schmidt A, Lukanidin E, Rabinovitch M. Interdependent serotonin transporter and receptor pathways regulate S100A4/Mts1, a gene associated with pulmonary vascular disease. *Circ Res*. 2005;97: 227–235.
6. Long L, MacLean M, Jeffery T, Morecroft I, Yang X, Southwood N, James V, Trembath R, Morrell N. Serotonin increases susceptibility to pulmonary hypertension in BMPR2-deficient mice. *Circ Res*. 2006;98: 818–827.
7. Altuvia Y, Landgraf P, Lithwick G, Elefant N, Pfeffer S, Aravin A, Brownstein MJ, Tuschl T, Margalit H. Clustering and conservation patterns of human microRNAs. *Nucleic Acids Res*. 2005;33:2697–2706.
8. Lee Y, Han J, Yeom KH, Jin H, Kim VN. Drosha in primary microRNA processing. *Cold Spring Harb Symp Quant Biol.* 2006;71:51–57.
9. Yeom KH, Lee Y, Han J, Suh MR, Kim VN. Characterization of DGCR8/Pasha, the essential cofactor for Drosha in primary miRNA processing. *Nucleic Acids Res.* 2006;34:4622–4629.
10. Lund E, Güttinger S, Calado A, Dahlberg JE, Kutay U. Nuclear export of microRNA precursors. *Science*. 2004;303:95–98.
11. MacRae IJ, Zhou K, Li F, Repic A, Brooks AN, Cande WZ, Adams PD, Doudna JA. Structural basis for double-stranded RNA processor by Dicer. *Science*. 2006;311:195–198.
12. Hammell CM. The microRNA-argonaute complex. *RNA Biol*. 2008;5: 123–127.
13. Selbach M, Schwanhäusser B, Thierfelder N, Fang Z, Khanin R, Rajewsky N. Widespread changes in protein synthesis induced by microRNAs. *Nature.* 2008;455:58–63.
14. Lujambio A, Calin GA, Villanueva A, Ropero S, Sánchez-Céspedes M, Blanco D, Montuenga LM, Rossi S, Nicoloso MS, Faller WJ, Gallagher WM, Eccles SA, Croce CM, Esteller M. A microRNA DNA methylation signature for human cancer metastasis. *Proc Natl Acad Sci U S A*. 2008;105:13556–13561.
15. Ambs S, Prueitt R, Ming Y, Hudson R, Howe T, Petrocca F, Wallace T, Liu C-G, Volinia S, Calin G, Yfantis H, Stephens R, Croce C. Genomic profiling of microRNA and messenger RNA reveals deregulated microRNA expression in prostate cancer. *Cancer Res*. 2008;68: 6162–6170.
16. Yang H, Kong W, He L, Zhao J-J, O'Donnell D, Wang J, Wenham R, Coppola D, Kruk P, Nicosia S, Cheng J. MicroRNA expression profiling in human ovarian cancer: miR-214 induces cell survival and cisplatin resistance by targeting PTEN. *Cancer Res*. 2008;68:425–433.
17. Thum T, Galuppo P, Wolf C, Fiedler J, Kneitz S, van Laake LW, Doevendans PA, Mummery CL, Borlak J, Haverich A, Gross C, Engelhardt S, Ertl G, Bauersachs J. MicroRNAs in the human heart: a clue to fetal gene reprogramming in heart failure. *Circulation*. 2007;116: 258–267.
18. Mann DL. MicroRNAs and the failing heart. *N Engl J Med*. 2007;356: 2644–2645.
19. Cheng Y, Ji R, Yue J, Yang J, Liu X, Chen H, Dean DB, Zhang C. MicroRNAs are aberrantly expressed in hypertrophic heart: do they play a role in cardiac hypertrophy? *Am J Pathol*. 2007;170:1831–1840.
20. Izzotti A, Calin GA, Arrigo P, Steele VE, Croce CM, De Flora S. Downregulation of microRNA expression in the lungs of rats exposed to cigarette smoke. *FASEB J.* 2009;23:806–812.
21. Breitling R, Armengaud P, Amtmann A, Herzyk P. Rank products: a simple, yet powerful, new method to detect differentially regulated genes in replicated microarray experiments. *FEBS Lett*. 2004;573:83–92.
22. Benjamini Y, Hochberg Y. Controlling the false discovery rate: a practical and powerful approach to multiple testing. *JRSS-B*. 1995;57: 289–399.
23. Wang Y, Weng T, Gou D, Chen Z, Chintagari NR, Liu L. Identification of rat lung-specific microRNAs by micoRNA microarray: valuable discoveries for the facilitation of lung research. *BMC Genomics.* 2007;8:29.
24. Brock M, Trenkmann M, Gay RE, Michel BA, Gay S, Fischler M, Ulrich S, Speich R, Huber LC. Interleukin-6 modulates the expression of the bone morphogenic protein receptor type II through a novel STAT3-microRNA cluster 17/92 pathway. *Circ Res*. 2009;104:1184–1191.
25. Long L, Crosby A, Yang X, Southwood M, Upton PD, Kim DK, Morrell NW. Altered bone morphogenetic protein and transforming growth factor-β signaling in rat models of pulmonary hypertension: potential for activin receptor-like kinase-5 inhibition in prevention and progression of disease. *Circulation*. 2009;119:566–576.
26. Gal H, Pandi G, Kanner A, Ram Z, Lithwick-Yanai G, Amariglio N, Rechavi G, Givol D. MIR-451 and imatinib mesylate inhibit tumor growth of glioblastoma stem cells. *Biochem Biophys Res Commun*. 2008; 376:86–90.
27. Grimson A, Srivastava M, Fahey B, Woodcroft BJ, Chiang HR, King N, Degnan BM, Rokhsar DS, Bartel DP. Early origins and evolution of microRNAs and Piwi-interacting RNAs in animals. *Nature*. 2008;455: 1193–1197.
28. Voelkel NF, Tuder RM. Cellular and molecular mechanisms in the pathogenesis of severe pulmonary hypertension. *Eur Respir J*. 1995;8: 2129–2138.
29. Voelkel N, Tuder R. Hypoxia-induced pulmonary vascular remodeling: a model for what human disease? *J Clin Invest*. 2000;106:733–738.
30. Ono S, Voelkel NF. PAF antagonists inhibit monocrotaline-induced lung injury and pulmonary hypertension. *J Appl Physiol*. 1991;71:2483–2492.
31. Laudi S, Steudel W, Jonscher K, Schoning W, Schniedewind B, Kaisers U, Christians U, Trump S. Comparison of lung proteome profiles in two rodent models of pulmonary arterial hypertension. *Proteomics*. 2007;7: 2469–2478.
32. Ji R, Cheng Y, Yue J, Yang J, Liu X, Chen H, Dean D, Zhang C. MicroRNA expression signature and antisense-mediated depletion reveal an essential role of microRNA in vascular neointimal lesion formation. *Circ Res*. 2007;100:1579–1588.
33. Davis BN, Hilyard AC, Lagna G, Hata A. SMAD proteins control DROSHA-mediated microRNA maturation. *Nature.* 2008;454:56–61.
34. Baek D, VillÃen J, Shin C, Camargo F, Gygi S, Bartel D. The impact of microRNAs on protein output. *Nature*. 2008;455:64–71.

Supplement Material

Supplement Methods

TaqMan q-PCR Analysis of Mature miRNAs and mRNAs

For the quantitative PCR (q-PCR), reactions were incubated in a 386-well optical plate at 95 C for 10 min, following by 40 cycles of 95 C for 15 s and 60 C for 1 min. Results were normalized to U87 or Rnu-48 values for miRNAs and to GAPDH for gene expression. The fold change for every miRNA or mRNA expression was obtained. The q-PCRs for each miRNA or mRNA were run in triplicate and results are presented as the mean ± standard deviation of samples. To assess the statistical significance of intergroup differences, a Student's *t* test was performed.

MiRNA extraction from frozen lungs, PASMCs, PAFs, PAECs and human serum and reverse transcription

Total RNA from tissues and cells were obtained using the miRNeasy kit (Qiagen, Hilden, Germany) following the manufacturer's instructions, treated with the DNAse 1, amplification grade (Sigma, St. Louis, MO, USA), to eliminate the genome DNA contamination and quantified using the NanoDrop ND-1000 Spectrophotometer (Nano-Drop Technologies, Wilmington, DE, USA). Absorbance of the RNA samples was quantified at 260 and 280 nm, and the 260/280 ratio was calculated. The samples showed a 260/280 ratio ≥ 1.9, which was assumed as an indicator of RNA purity. cDNA was synthesized from total RNA using stem-loop reverse transcription primers according to the TaqMan MicroRNA Assay protocol (Applied Biosystems, Foster city, CA, USA). Each reaction contained 50 ng of extracted total RNA, 50 nM stem-looped RT primer, 1 × RT buffer, 0.25 mM each of dNTPs, 3.33 U/μl Multiscribe reverse transcriptase and

0.25 U/μl RNase inhibitor. The 15 ml reactions were incubated in a 96-well plate for 30 min at 16 C, 30 min at 42 C, 5 min at 85 C and then held at 4 C.

miRNAs extraction from paraffin-embedded human lungs

The RecoverAll total RNA Isolation kit (Ambion, Streetsville, Canada) was used to extract total RNA (including miRNA) from FFPE samples. Three 10 μm slices were deparaffined with xylene for 3 min at 50℃, washed twice with ethanol, and digested with protease at 50℃ for 15 min, then for 15 min at 80° C. The lysate was passed through a filter cartridge and DNAse digested, then RNA was eluted in 30 μl of RNAse free water and quantified using the NanoDrop ND-1000 Spectrophotometer (Nano-Drop Technologies, Wilmington, DE, USA).

Primary Culture of Rat Pulmonary Artery Fibroblasts (PAFs)

Male Wistar rats (specific pathogen free, Harlan UK Ltd, 6 weeks old; 300-400g) were used throughout. Fibroblasts were prepared using the technique of Freshney [1].

Primary Culture of Rat Pulmonary Artery Smooth Muscle Cells (PASMCs)

Rat PASMCs were derived from small precapillary pulmonary arterioles using an iron oxide magnetic separation method, as previously described [2].

Primary Culture of Human Pulmonary Endothelial Cells (PAECs)

Human Pulmonary Endothelial Cells were obtained from Lonza (Lonza Group Ltd, Basel, Switzerland) and cultured by following the Supplier's instructions.

Growth of Cells in a Hypoxic Environment

A humidified temperature-controlled incubator (Galaxy R model, Wolf Laboratories, UK) was used as a hypoxic chamber. This incubator allows control of internal oxygen levels between 0 and 21% while CO_2 level is simultaneously controlled at 5%.

Western Blot Analysis

Rat lung tissues removed from control and 7 day monocrotaline-treated male Sprague-Dawley rats were homogenated in lysis buffer containing 150 mM NaCl, 20 mM Tris HCl pH 7.5, 1 mM EDTA, 1 mM EGTA, 1% Triton X 100, 2.5 mM napyrophosphate, 1 mM phenylmethylsulfonylfluoride (PMSF), 1 mM Na_3VO_4, 1 mM βglycerophosphate and 1 μg/ml leupeptin. The homogenates were sonicated and incubated 20 min on ice. Lysed tissues were centrifuged at 14,000 rpm at 4℃ for 1 5 min. The protein content was determined using a BCA assay (Pierce, Rockford, IL, USA). After blocking in TBS–Tween 0.1%–Milk 10%, filter was incubated with an anti-TGFBR1 antibody (Santa Cruz Biotechnology Inc.) overnight at 4℃. The membrane was then incubated with secondary antibody (dilution 1:1000, goat anti-rabbit Abcam, Cambridge, UK) for 1 hour at room temperature. The ECL Western Blotting detection kit (Amersham, Little Chalfont, UK) was used to detect the presence of the protein of interest on the membrane. Equal sample loading was verified by stripping the blot and reprobing it with an anti-β-actin antibody (Abcam, Cambridge, UK). Protein quantification was performed with the Scion Image software (www.scioncorp.com): band intensities of the protein of interest were established and normalized to the relative β actin signal.

Immunohistochemistry

Rat lungs were fixed in 4% paraformaldehyde solution at 4^0C for 18 hours and embedded in paraffin. After deparaffinization with graded concentrations of xylene and

ethanol, slides were immersed in 3% H_2O_2 in phosphate buffered saline (PBS) for 30 minutes at room temperature to block endogenous peroxidase activity. Then, they were incubated with 20% normal goat serum for 30 minutes to reduce non-specific background staining. The sections were then incubated with rabbit anti-TGFBR1 antibody (Abcam, Cambridge, UK) at 4 μg/ml or isotype matched rabbit IgG nonimmune control (Dako, High Wycombe, UK). Sections were then incubated with appropriate biotinylated secondary antibody (Dako, High Wycombe, UK) diluted 1:200 in 1% (w/v) BSA in PBS, and then horseradish peroxidase-labelled Extravidin™ (Sigma, St. Louis, MO, USA) diluted 1:400 in 1% (w/v) BSA in PBS. Colour was developed using 3.3 diaminobenzidine-nickel and the nuclei were counterstained with Mayer's haematoxylin.

Statements

Animal procedures were conducted in accordance with the United Kingdom Animals (Scientific Procedures) Act 1986 (Home Office license PPL60/3773) and with the "Guide for the Care and Use of Laboratory Animals" published by the US National Institutes of Health (NIH publication No. 85-23, revised 1996).

References

1. Freshney R. *In: Cultures of animals cells.* 1983:99–118.
2. Sobolewski A, Jourdan KB, Upton PD, Long L, Morrell NW. Mechanism of cicaprost-induced desensitization in rat pulmonary artery smooth muscle cells involves a PKA-mediated inhibition of adenylyl cyclase. *Am J Physiol Lung Cell Mol Physiol* 2004;287:L352-359.

Supplement Figure Legends

Supplement Figure I. Global miRNA profiling. (A) Design of the miRNA microarray study investigating PAH in hypoxic or monocrotaline-exposed rats. Each circle represents animal groups (minimum n = 5/group), with each hypoxia treatment being in red and each drug treatment in blue. The control group is represented in green. Each arrow represents a two-channel microarray experiment. (B) Heat map showing the expression level of all miRNA in the global profiling protocol. Refer to Supplement Table 1 for complete microarray dataset.

Supplement Figure II. q-PCR curves showing DICER and DROSHA expression level in the lung of hypoxic or monocrotaline-injected six weeks male rats. (A) *In vivo* q-PCR result showing the dysregulation of both DICER and DROSHA after a hypoxic/monocrotaline treatment. For every gene, the time point with the maximum dysregulation for both the models has been chosen and the results are showed in duplicate. (B) *In vitro* q-PCR result showing DICER downregulation in 24 hours hypoxic rat PAFs versus untreated cells. The q-PCR curves are shown in duplicate.

Supplement Figure III. q-PCR curves showing miRNA expression levels in the lung of hypoxic or monocrotaline-injected six weeks male rats. For every miRNA, the time point with the maximum dysregulation for both the models has been chosen and the results are showed in triplicate. One example of amplification curve has been chosen for miR-145, taken as negative control.

Supplement Figure IV. Validation of miR-17/92 cluster in hypoxic and monocrotaline rats. q-PCR analysis of hypoxic and monocrotaline-injected rats after 2, 7 and 21 days of exposition. Total RNA was extracted in quadruplicate from hypoxic (grey bars) or monocrotaline-injected (black bars) six weeks male rats. Time

points and samples were tested in triplicate. Results were normalized to U87 values and expressed as relative fold change, with an arbitrary value of 1 assigned to the control group. (*p<0.05, **p<0.005, ***p<0.001 vs control samples).

Supplement Figure V. miRNA expression is regulated by hypoxia *in vitro* in human cells. (A and B) q-PCR analysis of hypoxic fetal human PAFs (A) and human PAECs (B) showing the expression level of miR-21, miR-22, miR-30c and let-7f after 24 hours of stimulation. These experiments were performed with total RNA extracted from both the control and the hypoxic cells. Results were normalized to Rnu-48 values and expressed as relative fold change, with an arbitrary value of 1 assigned to the control group (*p<0.05, ***p<0.001 vs control samples).

Supplement Figure VI: Assessment of miRNA target mRNA levels in rat lung following hypoxic and monocrotaline injuries. Total RNA was extracted from lung samples of hypoxic (grey bars) and monocrotaline-treated (black bars) rats. cDNA was prepared and mRNA levels were assessed by TaqMan analysis and plotted as fold change vs control samples. Results were normalized to GAPDH values. The miRNAs that possess predicted seed sequences for each target are indicated. (*p<0.05, **p<0.005, ***p<0.001 vs control samples).

Supplement Table I. Absolute levels of miRNAs modulated during the progression of PAH. Values are means and standard deviations for miRNA of the intensities for each condition (at least n=5/group).

Supplement Table II. Absolute levels of selected miRNAs. Raw values for miRNAs up- and down-regulated in PAH rats are shown.

Supplement Table III. Absolute levels of miR-17/92 cluster. Raw values for miR-17/92 cluster in PAH rats are shown.

Supplement Table IV. Predicted targets for the three downregulated miRNAs miR-21, miR-22 and miR-30c. A list of potential targets for miR-21, miR-22 and miR-30c, obtained through bioinformatic tools, is shown.

Supplement Table V. Predicted targets for the two up-regulated miRNAs miR-451 and miR-322. A list of potential targets in common between the two miRNAs, obtained through bioinformatic tools is shown. Proteins marked in red have been show to be targets also of the down-regulated miRNA group.

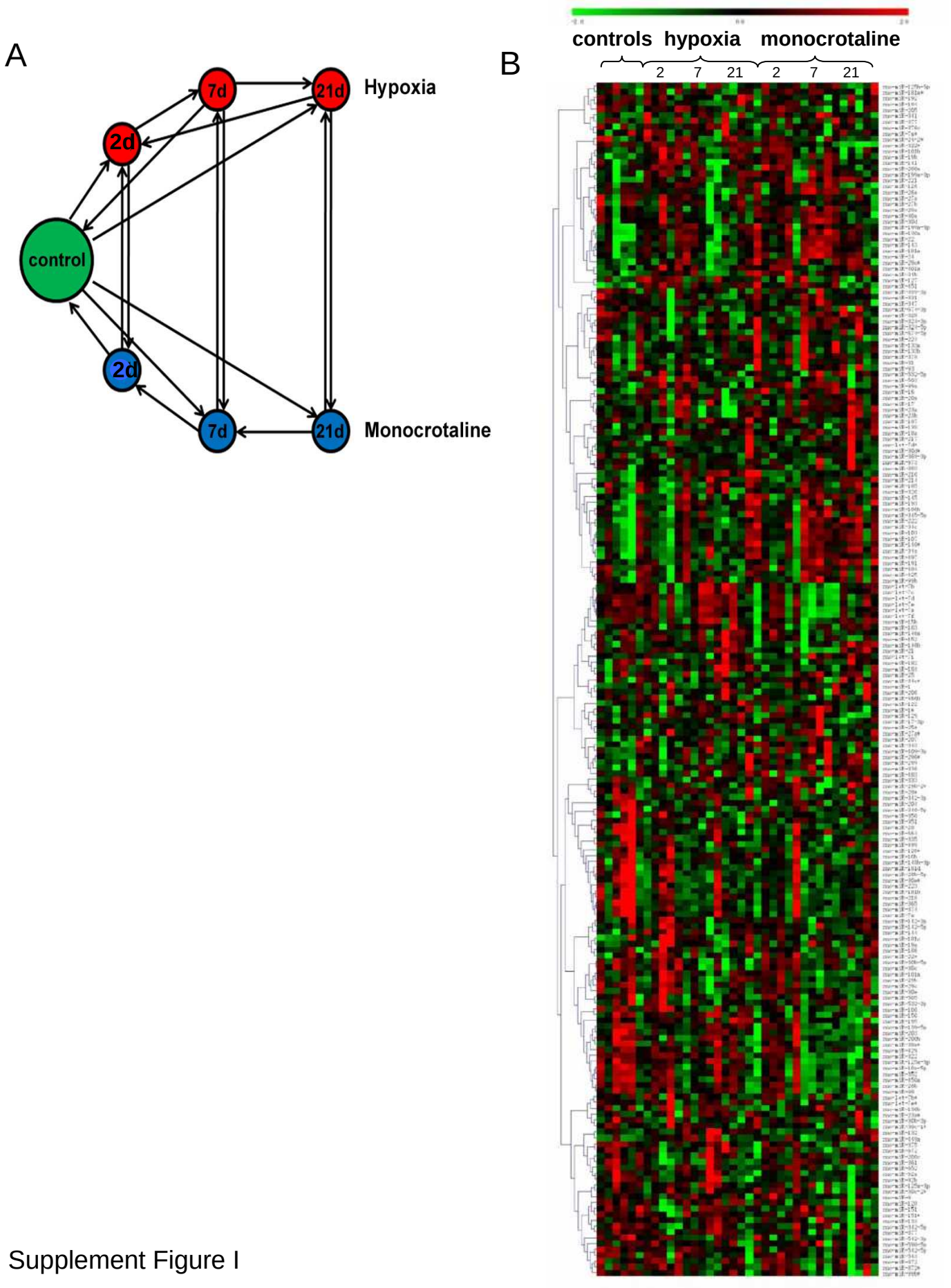

Supplement Figure I

A

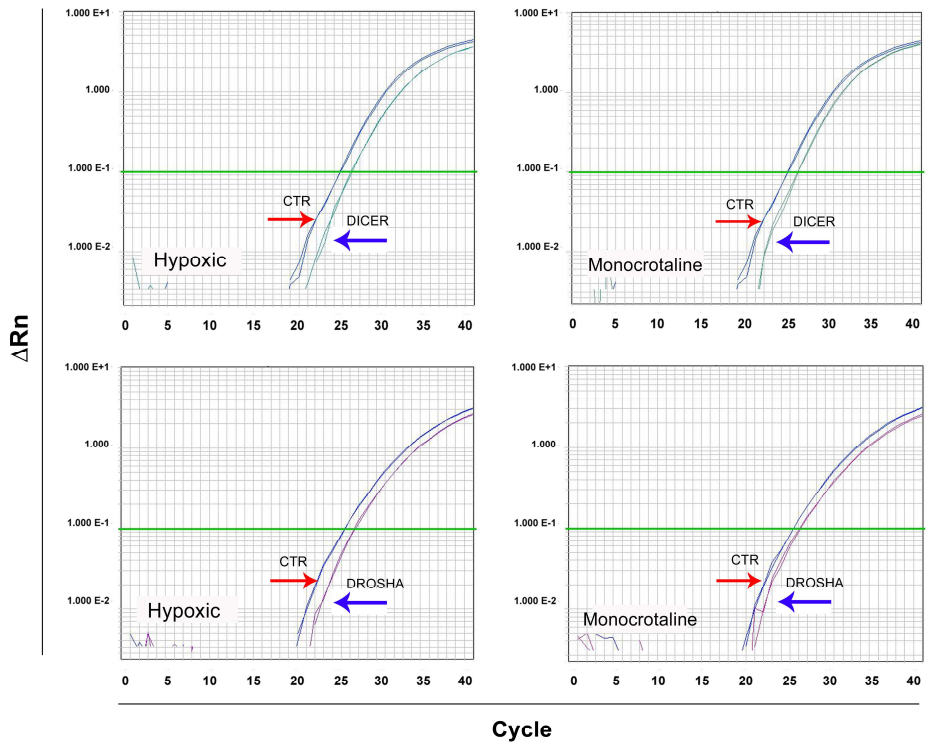

B

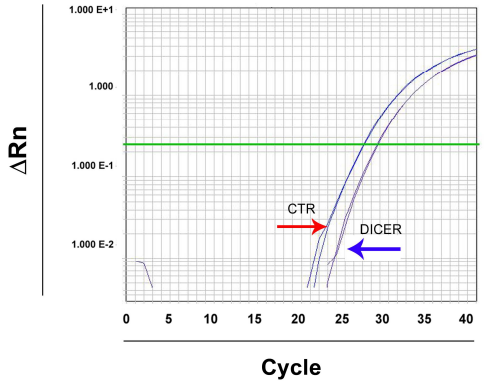

Supplement Figure II

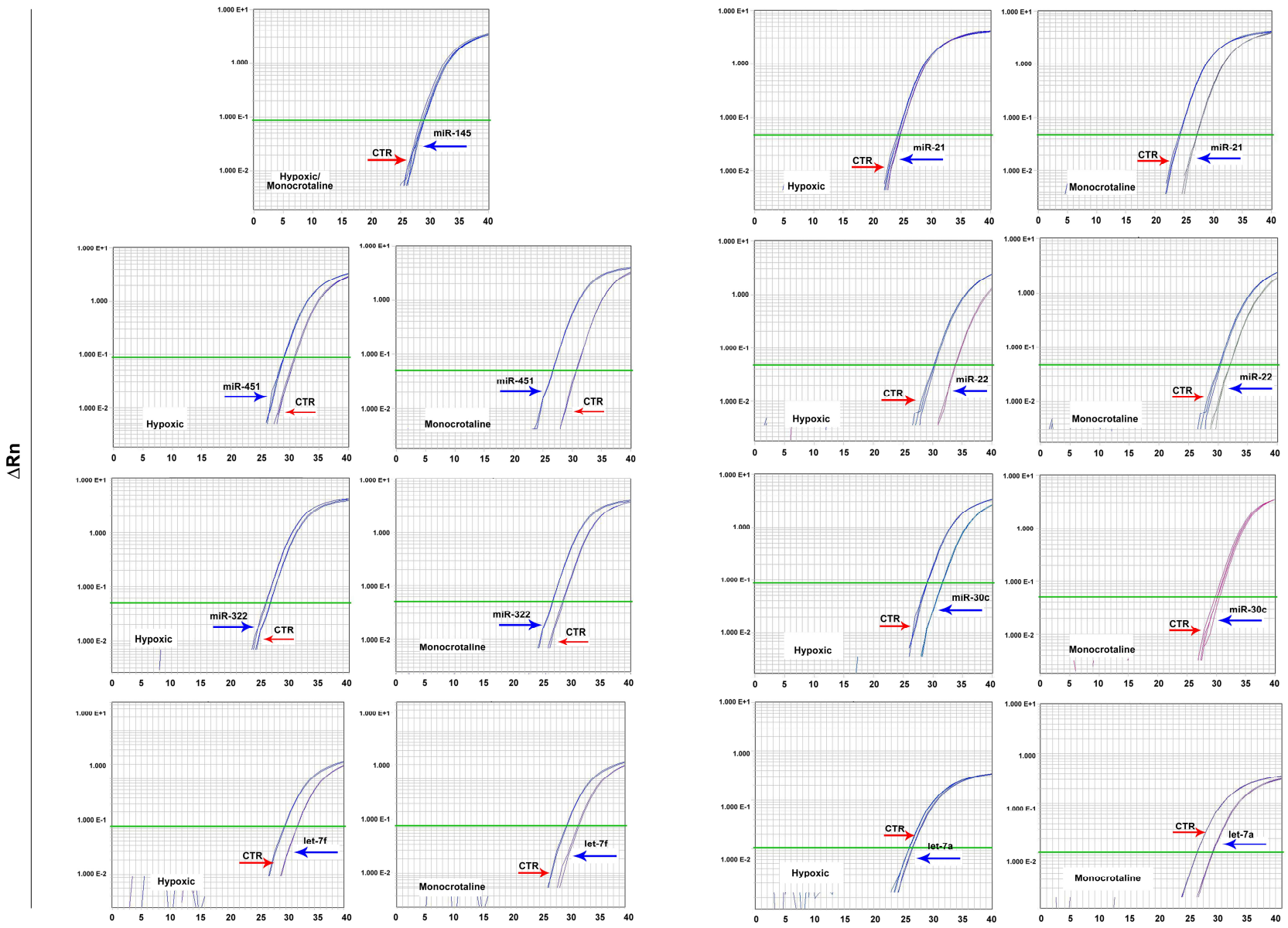

Supplement Figure III

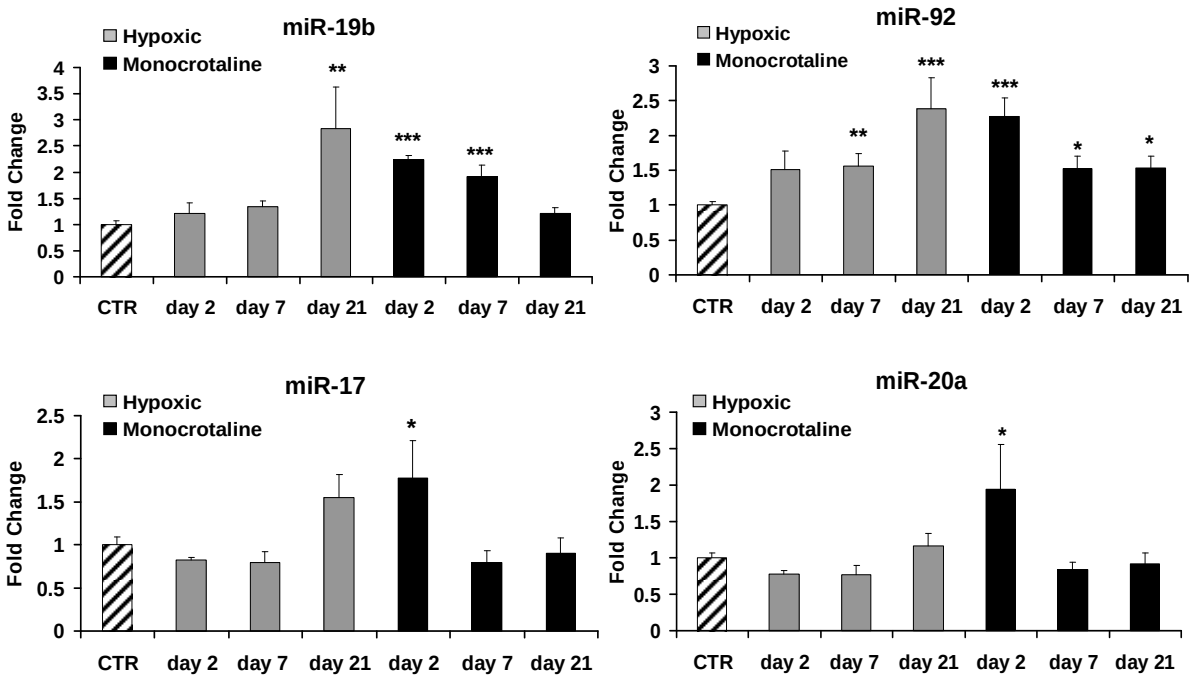

Supplement Figure IV

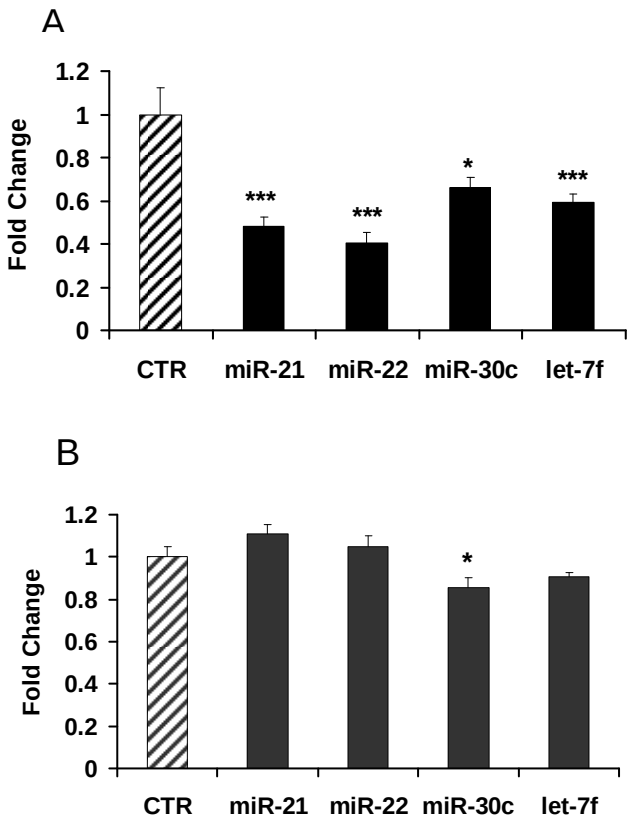

Supplement Figure V

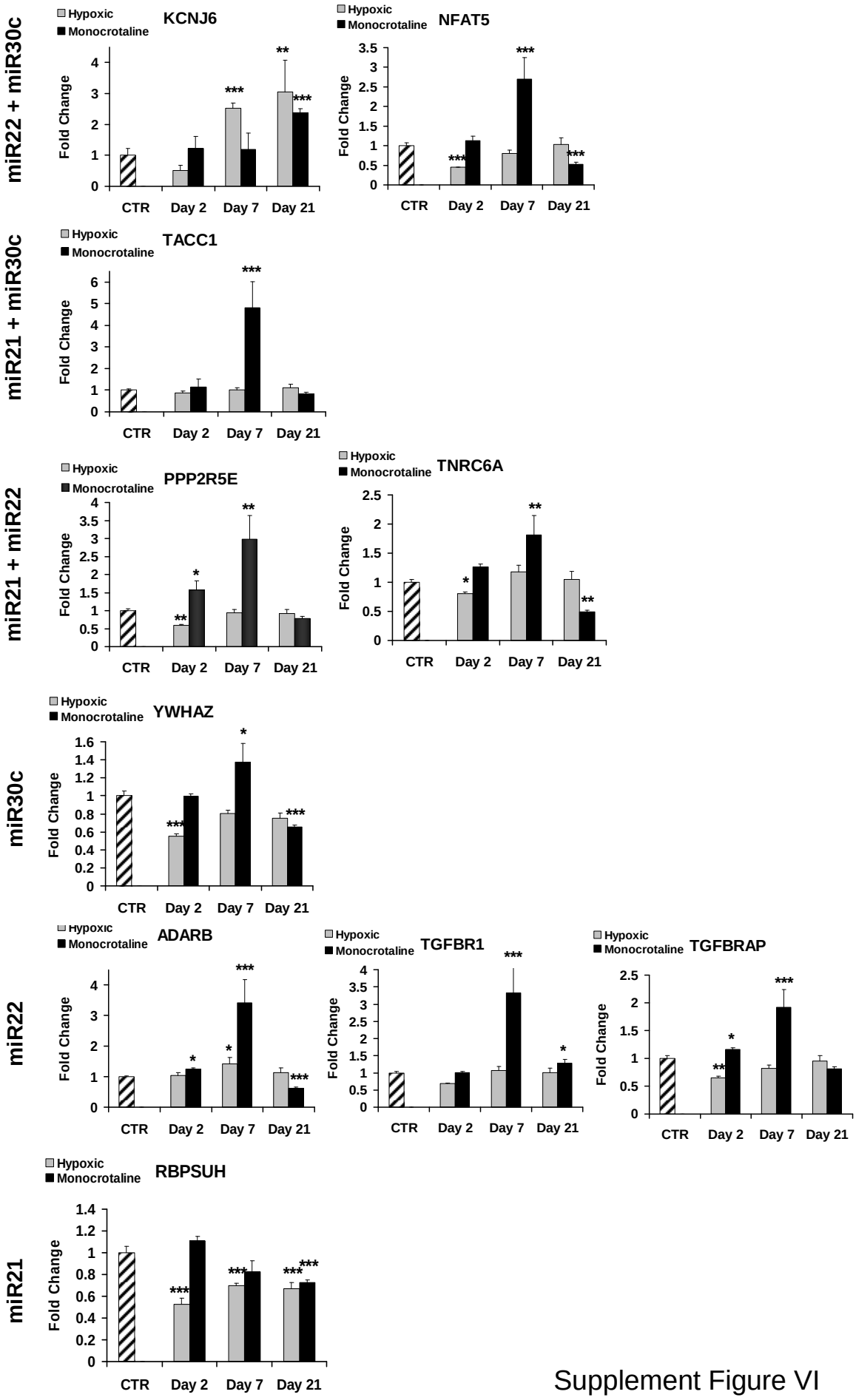

Supplement Figure VI

Supplement Table I. Absolute levels of miRNAs modulated during the progression of PAH

	Group 1 control		Group 2 Hypoxiaday 2		Group 3 Hypoxia day 7	
Reporter Name	Mean	StDev	Mean	StDev	Mean	StDev
rno-miR-322	1,066	326	1,109	345	931	484
rno-miR-451	467	188	1,528	405	996	388
rno-miR-21	1,686	739	1,862	594	1,840	1,126
rno-let-7f	8,290	870	7,094	2,842	8,257	2,295
rno-let-7a	9,747	1,309	8,573	3,011	10,983	3,372
rno-miR-26b	2,709	1,131	2,034	906	1,349	882
rno-miR-30b-5p	3,716	1,037	3,964	1,161	2,526	898
rno-let-7d	6,525	638	5,423	2,355	7,001	2,474
rno-miR-30c	4,085	849	4,285	982	3,181	980
rno-miR-125a-5p	2,232	849	1,515	244	1,903	1,006
rno-miR-30d	1,810	489	2,087	660	1,411	490
rno-let-7c	8,762	1,669	7,642	2,817	10,755	3,730
rno-miR-92b	309	107	204	50	370	210
rno-miR-30e	535	288	758	413	277	145
rno-miR-30a	2,082	669	2,517	1,022	1,415	662
rno-miR-99a	294	70	439	99	344	89
rno-miR-22	333	225	720	302	638	445
rno-miR-126	11,056	2,611	12,492	1,942	10,000	3,716
rno-miR-29c	594	362	521	345	219	164
rno-miR-92a	567	188	445	85	715	337
rno-miR-214	306	178	285	103	927	976
rno-miR-191	1,535	257	1,526	423	1,500	543
rno-let-7b	7,268	1,534	6,182	2,558	9,176	3,568
rno-miR-146b	344	128	322	30	380	90
rno-miR-24	2,724	875	3,264	867	3,218	1,904
rno-miR-361	383	100	233	68	362	179
rno-miR-140*	215	132	167	64	259	90
rno-miR-222	223	129	243	84	306	91
rno-miR-29a	2,271	704	2,324	879	1,542	638

rno-miR-221	222	61	322	56	291	120
rno-miR-143	1,870	775	2,597	817	2,229	1,238
rno-miR-130a	250	110	422	139	375	165
rno-miR-497	295	270	296	164	684	606
rno-miR-322*	106	16	115	16	99	23
rno-miR-210	21	8	32	9	54	19
rno-miR-449a	47	26	69	10	156	116
rno-miR-132	26	5	28	5	57	31
rno-miR-19b	75	23	223	153	110	56
rno-miR-151*	108	20	74	26	110	23
rno-miR-301a	18	5	42	22	20	14
rno-miR-100	200	53	259	89	170	53
rno-miR-652	106	46	79	24	152	128
rno-miR-101a	65	25	123	112	48	19
rno-miR-336	9	6	8	4	14	5
rno-miR-101b	43	12	84	28	47	22
rno-miR-347	13	2	9	4	13	4
rno-miR-184	17	9	15	4	26	22
rno-miR-129	11	3	17	7	13	4
rno-miR-429	245	76	217	39	181	82
rno-miR-151	905	188	606	194	866	177
rno-miR-195	3,062	423	3,110	183	2,940	469
rno-miR-664	64	41	19	5	35	31
rno-miR-26a	11,526	2,405	11,447	1,603	9,172	2,742
rno-let-7e	2,978	1,147	2,338	1,645	3,034	1,400
rno-miR-872*	25	9	31	8	19	5
rno-miR-34a	296	261	245	112	496	431
rno-miR-200b	1,161	283	781	267	972	318
rno-miR-138	11	4	14	4	12	3
rno-miR-205	39	14	42	10	40	9
rno-miR-328	48	13	32	12	39	10
rno-miR-352	664	406	465	361	379	382
rno-miR-181a	650	287	866	194	654	397

rno-miR-144	10	3	23	16	12	5
rno-miR-193	17	6	20	7	26	7
rno-miR-34b	23	7	37	8	32	17
rno-miR-28	147	60	96	13	98	36
rno-miR-10a-5p	525	272	264	112	293	275
rno-miR-375	692	144	431	144	535	165
rno-miR-199a-5p	74	39	149	23	131	69
rno-miR-29b	75	46	122	99	36	15
rno-miR-133a	43	25	39	11	46	16
rno-miR-450a	539	431	235	219	211	372
rno-miR-139-5p	62	39	36	8	50	22
rno-miR-15b	726	252	710	220	1,045	482
rno-miR-29b-2*	19	4	17	6	16	4
rno-miR-98	772	866	501	634	225	194
rno-miR-203	103	67	49	16	61	23
rno-miR-877	19	5	13	6	23	9
rno-miR-126*	266	497	283	478	34	17
rno-miR-103	481	271	465	164	562	193
rno-miR-200c	1,295	301	906	273	1,604	784
rno-miR-365	125	105	37	21	45	53
rno-miR-185	195	75	137	47	181	51
rno-miR-345-5p	44	29	30	12	51	28
rno-miR-34c	63	47	68	24	76	35
rno-miR-324-5p	35	11	28	12	34	7
rno-miR-374	77	70	34	25	28	25
rno-miR-1*	10	3	11	5	13	3
rno-miR-17	199	29	240	75	256	85
rno-miR-340-5p	24	19	11	4	13	2
rno-miR-199a-3p	709	182	999	178	782	259
rno-miR-217	15	2	12	3	16	3
rno-miR-200a	211	80	340	83	197	132
rno-miR-107	427	226	427	151	507	171
rno-miR-30a*	145	66	108	31	125	57

rno-miR-125a-3p	24	6	21	5	28	9
rno-miR-542-5p	26	10	19	6	22	7
rno-miR-218	253	221	99	71	77	86
rno-miR-150	1,551	399	1,490	154	1,687	326
rno-miR-25*	20	4	17	5	19	5
rno-miR-7a	53	48	18	9	29	34
rno-miR-299	11	4	11	4	13	6
rno-miR-23a	6,618	738	7,458	2,151	6,186	2,028
rno-miR-499	18	13	11	4	10	6
rno-miR-204	20	10	10	3	14	6
rno-miR-127	18	6	26	5	19	8
rno-miR-335	38	35	20	9	21	14
rno-miR-378	73	46	67	22	70	22
rno-miR-99b	577	210	580	185	705	246
rno-miR-324-3p	27	5	23	9	25	7
rno-miR-187	28	8	21	7	34	8
rno-miR-106b	179	59	183	57	211	51
rno-miR-341	11	3	22	17	16	5
rno-miR-20a	245	27	256	48	266	33
rno-miR-99b*	11	3	10	4	7	2
rno-miR-223	173	150	104	87	96	110
rno-miR-409-3p	15	6	16	7	21	11
rno-miR-181b	111	95	61	45	52	47
rno-miR-128	120	20	97	27	126	17
rno-miR-142-5p	21	11	41	38	13	7
rno-miR-30e*	98	79	49	38	45	49
rno-miR-30c-2*	37	5	37	9	39	12
rno-miR-145	4,950	1,562	5,756	2,691	7,329	4,154
rno-miR-20b-5p	71	49	56	45	37	30
rno-miR-141	73	33	114	29	68	40
rno-miR-224	81	26	61	15	74	7
rno-miR-122	22	10	22	14	29	13
rno-let-7i	4,293	240	4,112	375	3,991	375

rno-miR-342-5p	33	9	20	8	32	11
rno-miR-133b	37	18	39	7	41	13
rno-miR-31	80	37	65	16	66	25
rno-miR-186	23	10	34	22	19	8
rno-miR-672	153	69	108	57	160	117
rno-miR-503	21	5	28	11	25	7
rno-miR-34c*	134	71	127	55	139	57
rno-miR-181c	19	12	30	16	18	5
rno-miR-18a	23	5	25	9	27	4
rno-miR-542-3p	43	39	24	12	14	11
rno-miR-16	4,051	727	4,686	672	4,517	578
rno-miR-543	15	8	16	11	10	3
rno-miR-23b	6,669	830	7,210	2,081	6,128	2,003
rno-miR-146a	552	223	491	70	515	210
rno-miR-152	236	81	253	63	241	84
rno-miR-28*	50	13	44	8	52	4
rno-miR-181d	70	62	53	35	31	14
rno-miR-343	12	6	11	3	14	4
rno-miR-7a*	17	10	29	26	14	6
rno-miR-872	74	21	86	22	60	6
rno-miR-296*	16	5	18	7	20	10
rno-miR-1	20	13	120	218	14	5
rno-miR-9	10	3	10	6	12	8
rno-miR-142-3p	17	13	25	20	13	6
rno-miR-351	34	23	22	6	21	6
rno-miR-331	37	16	28	13	28	6
rno-miR-29c*	23	4	28	5	26	7
rno-miR-22*	36	11	43	14	35	11
rno-miR-505	33	16	33	14	23	7
rno-miR-23a*	20	3	19	10	24	5
rno-miR-350	25	13	25	10	18	5
rno-miR-10b	42	52	28	26	23	9
rno-miR-24-2*	100	36	105	27	85	28

rno-let-7e*	13	2	20	18	13	2
rno-miR-425	102	47	95	36	107	37
rno-miR-194	40	6	40	7	31	5
rno-miR-192	35	10	36	13	28	7
rno-miR-674-5p	97	30	66	26	88	33
rno-miR-30d*	11	1	14	8	11	3
rno-let-7b*	20	5	30	22	19	5
rno-miR-148b-3p	53	40	38	13	34	9
rno-miR-130b	20	7	24	11	22	4
rno-miR-182	78	33	90	61	79	19
rno-miR-483	12	5	11	3	13	8
rno-miR-333	21	8	19	5	22	9
rno-miR-134	14	2	14	3	16	6
rno-miR-183	88	14	98	40	107	12
rno-miR-466b	11	3	11	8	9	4
rno-miR-207	11	6	30	42	14	4
rno-miR-320	643	303	507	151	728	252
rno-miR-532-3p	21	14	27	18	15	7
rno-miR-181a*	18	7	20	9	19	4
rno-miR-674-3p	46	10	38	13	39	7
rno-miR-598-5p	9	3	10	6	9	3
rno-miR-484	21	8	18	9	20	8
rno-miR-17-3p	14	4	13	4	13	3
rno-miR-342-3p	134	96	74	27	101	59
rno-miR-27a*	10	2	12	8	11	3
rno-miR-125b-5p	3,117	675	3,445	343	3,312	868
rno-let-7d*	32	20	37	24	22	2
rno-miR-30c-1*	15	4	17	10	16	3
rno-miR-27b	1,325	564	1,394	526	1,071	372
rno-miR-883	9	5	8	4	8	2
rno-miR-27a	1,534	653	1,443	548	1,135	525
rno-miR-25	555	127	481	71	570	156
rno-miR-376c	8	5	8	3	10	2

rno-miR-339-3p	21	9	17	9	15	3
rno-miR-19a	12	2	21	14	14	3
rno-miR-673	9	4	9	4	10	3
rno-miR-93	118	63	118	33	136	66
rno-miR-369-3p	9	5	9	4	8	2
rno-miR-30b-3p	25	6	22	8	21	3
rno-miR-377	86	109	428	619	201	337
rno-miR-206	15	4	15	7	14	2
rno-miR-532-5p	19	4	19	9	20	5

Group 4		Group 5		Group 6		Group 7	
Hypoxia day 21		MCT day 2		MCT day 7		MCT day 21	
Mean	StDev	Mean	StDev	Mean	StDev	Mean	StDev
834	541	832	309	210	83	241	285
1,539	928	1,008	462	1,335	449	479	187
2,243	1,515	1,276	595	367	141	2,881	1,809
6,035	3,257	7,401	2,801	2,560	485	6,359	1,982
8,370	3,371	8,926	2,822	4,038	585	8,414	1,567
1,294	962	2,300	1,199	451	89	1,142	1,251
2,198	760	4,154	527	3,001	733	2,624	740
5,241	3,148	5,922	2,275	2,262	584	4,962	2,137
2,673	763	4,120	468	3,300	495	2,918	492
1,147	507	1,652	744	758	142	1,221	514
1,618	399	1,860	346	2,613	411	1,458	215
9,467	4,038	8,240	1,813	4,809	554	8,983	1,339
159	37	236	61	203	23	223	73
402	132	580	91	429	154	340	166
2,026	665	2,296	452	2,889	350	1,494	485
290	89	404	117	444	81	280	83
680	337	570	355	1,107	137	666	189
12,414	4,410	11,342	3,751	15,687	3,943	7,308	2,378

293	165	438	216	130	34	268	282
381	89	484	111	401	52	434	111
509	313	271	115	426	113	687	304
1,486	341	1,458	438	2,386	667	2,427	874
8,378	4,715	6,913	1,770	3,788	1,051	7,290	1,285
515	339	284	37	275	102	604	174
3,580	1,408	3,261	1,271	6,051	1,494	3,763	1,233
243	23	328	71	321	62	371	73
433	256	201	105	408	150	312	117
270	132	255	83	425	113	477	183
2,322	592	2,364	469	3,087	541	1,949	485
318	64	344	109	372	118	424	69
3,412	1,452	2,218	811	4,281	998	2,159	708
443	210	479	247	687	259	429	109
695	478	340	209	812	204	496	200
119	5	111	14	90	11	62	7
124	89	20	4	33	4	28	8
48	12	69	30	43	17	105	38
33	4	22	4	24	2	35	14
140	40	155	33	147	66	88	39
84	12	91	23	92	32	60	24
27	7	36	12	20	6	35	12
167	41	176	40	145	24	150	34
72	12	118	21	78	29	57	13
62	26	79	25	30	11	50	36
18	12	13	4	19	9	15	4
59	25	75	15	46	18	45	24
12	3	12	2	28	29	10	4
39	26	16	6	13	4	21	9
17	9	13	5	21	10	8	5
144	82	260	36	149	55	144	75
767	101	693	104	876	282	674	138
3,494	746	3,272	540	2,864	305	2,420	786

15	9	40	40	34	24	23	14
10,994	5,024	10,736	3,871	17,943	2,717	11,200	4,091
2,145	1,680	2,592	1,541	848	346	2,371	1,841
21	6	30	3	17	7	22	13
423	224	294	187	508	156	659	243
738	312	1,048	326	705	109	772	199
14	4	13	3	10	4	27	22
29	6	46	6	26	8	33	15
30	8	29	4	43	9	46	16
215	188	477	442	99	77	237	240
898	396	759	287	1,415	355	702	227
13	3	13	3	10	3	12	3
32	13	18	4	28	14	29	13
43	25	52	27	38	9	43	19
80	10	106	58	79	12	86	15
252	115	306	194	127	38	222	147
538	452	586	149	402	114	344	117
212	182	117	76	153	38	128	36
81	28	79	38	43	12	70	43
80	76	46	32	189	237	39	13
162	162	287	366	39	25	90	130
42	23	64	28	23	8	29	16
627	446	715	160	444	144	914	253
17	5	22	3	14	7	23	7
272	365	663	842	38	28	547	1,099
54	29	78	49	35	7	55	36
15	5	18	5	11	6	16	7
38	15	277	435	32	15	58	74
609	238	487	136	787	176	730	246
1,096	300	1,181	219	1,180	242	1,195	155
23	10	61	78	22	7	33	14
240	83	150	13	187	63	214	68
72	58	41	14	90	47	55	25

136	142	97	72	144	75	123	48
46	31	33	7	52	17	49	22
18	9	44	55	17	5	28	17
11	5	13	5	20	14	9	3
180	40	193	44	249	43	234	42
12	5	12	4	12	4	12	3
1,012	160	851	206	992	313	854	143
30	33	17	4	19	6	22	9
223	96	397	232	296	144	186	50
564	220	457	124	677	118	665	216
100	36	140	47	87	17	86	24
20	3	22	6	20	10	16	5
18	9	17	6	16	6	13	6
92	49	106	100	37	13	76	46
1,405	336	1,383	321	1,197	229	1,257	348
18	6	17	7	218	438	17	6
15	8	31	41	9	3	28	27
24	22	15	5	19	13	21	8
6,426	2,851	7,137	1,357	8,079	364	9,313	2,855
9	4	12	6	8	2	14	6
11	2	10	6	12	5	12	5
19	4	19	8	20	10	14	5
15	3	18	8	13	5	13	3
96	44	75	21	195	221	80	27
546	186	534	98	885	266	700	251
29	14	25	5	36	5	29	9
33	17	29	11	23	5	33	14
221	51	175	38	253	35	218	61
19	13	18	5	26	13	15	5
211	68	239	21	257	20	271	52
8	5	11	3	6	3	10	13
56	27	107	64	49	21	84	41
12	4	20	8	26	14	14	5

35	12	56	45	26	8	41	12
115	31	102	21	90	23	100	43
18	5	20	3	22	20	22	9
31	5	66	71	29	9	42	16
39	8	41	7	31	10	30	11
8,116	4,638	6,097	3,380	9,359	1,975	7,536	2,748
25	5	45	32	28	8	33	8
77	27	95	32	89	32	72	14
88	20	66	16	78	30	65	20
243	481	22	13	26	7	24	13
4,674	1,006	4,241	318	4,759	991	4,577	422
25	5	27	12	25	9	26	13
69	56	43	27	128	151	38	17
122	70	79	37	97	51	69	24
24	12	25	4	18	6	28	12
157	159	143	47	64	20	130	72
19	7	18	3	22	6	19	7
157	25	148	24	133	65	213	75
19	8	21	4	18	5	19	4
27	9	20	8	26	8	31	9
29	30	19	17	12	4	20	18
4,333	1,100	4,895	1,071	5,076	611	4,758	676
8	5	16	8	8	4	7	5
6,101	2,783	6,887	1,087	6,951	1,004	8,485	2,170
774	464	606	229	395	177	496	81
279	139	269	39	193	81	177	60
46	21	51	9	40	15	41	9
30	13	52	42	25	14	33	10
13	5	14	3	19	11	12	4
22	18	13	4	12	5	19	7
72	27	85	16	62	17	71	30
27	18	21	9	31	23	29	13
41	40	27	27	48	39	57	78

9	6	33	51	7	2	8	5
14	4	16	6	10	5	15	4
20	11	23	5	22	4	21	7
30	12	27	4	38	13	29	3
29	9	29	5	31	8	30	8
32	9	45	12	33	7	37	10
26	8	34	8	29	9	31	11
23	5	18	3	22	2	23	11
19	6	20	3	18	2	20	2
21	7	27	27	13	4	16	6
98	27	104	15	93	28	78	6
13	4	13	3	11	4	11	2
107	37	81	19	134	44	126	57
42	20	41	3	35	8	35	14
44	25	31	6	27	13	36	16
90	46	85	12	93	37	114	66
42	65	11	2	16	3	249	533
16	3	23	8	20	10	18	9
27	11	41	17	28	14	38	21
17	4	17	4	22	7	19	4
92	33	66	7	62	23	92	39
18	6	14	10	19	13	16	7
19	3	28	13	18	7	24	10
13	4	15	3	17	12	10	4
126	103	96	33	79	30	113	18
13	12	10	3	7	4	14	9
16	11	15	6	17	7	16	5
665	321	626	112	740	212	691	224
16	3	19	5	17	5	18	11
15	5	22	4	20	4	19	9
36	9	37	8	44	12	52	29
7	6	9	2	16	15	6	4
18	6	17	10	24	4	19	5

14	5	16	2	21	20	12	5
87	103	98	49	57	18	200	309
10	3	10	2	16	10	11	5
2,825	389	3,383	499	3,355	609	3,191	1,291
53	70	23	5	25	12	141	266
15	6	13	1	13	6	14	7
1,298	290	1,134	126	1,093	224	1,119	220
10	3	8	4	9	8	35	61
1,278	569	1,153	78	1,297	255	1,138	443
570	219	512	88	595	129	594	117
10	13	9	4	7	3	6	2
14	9	15	5	24	26	13	7
15	7	14	3	15	8	15	5
11	4	9	4	21	32	38	65
136	88	100	27	154	61	137	96
11	7	8	3	7	3	27	44
23	6	23	3	24	5	22	8
236	457	73	96	703	1,429	90	124
26	28	12	2	18	13	20	14
19	6	17	3	23	14	20	8

Supplement Table II. Absolute levels of selected miRNAs

miRNA	CTR	H day 2	H day 7	H day 21	M day 2	M day 7	M day 21
rno-let-7a	7,729	9,439	14,993	9,542	11,972	3,058	10,101
	10,540	11,385	13,685	8,116	5,174	4,613	6,258
	8,832	11,260	10,171	12,824	6,837	4,200	7,714
	9,897	5,651	6,613	7,891	10,664	4,272	8,240
	10,024	5,129	9,454	3,476	9,985	4,045	9,757
	11,458						
rno-let-7f	6,718	7,552	10,733	6,326	10,128	1,738	8,560
	8,821	9,485	9,582	6,160	3,212	2,697	3,729
	8,120	10,117	8,605	11,080	6,055	2,544	5,583
	9,046	4,176	4,690	4,297	9,375	2,872	8,108
	8,112	4,141	7,675	2,312	8,233	2,947	5,813
	8,923						
rno-miR-322	1,194	643	579	816	876	169	211
	1,136	1,386	546	1,142	300	354	71
	1,413	1,188	1,647	1,563	889	194	94
	872	1,457	667	215	1,072	142	742
	1,271	872	1,216	436	1,023	193	89
	508						
rno-miR-21	2,201	1,037	2,010	3,491	1,315	439	3,279
	2,423	2,470	919	2,304	368	508	1,153
	1,508	2,399	3,712	3,972	1,204	354	2,525
	899	1,795	1,104	606	1,475	137	5,773
	2,326	1,607	1,455	844	2,015	399	1,676
	757						
rno-miR-22	386	770	526	512	372	1,118	639
	128	286	314	576	1,114	1,199	878
	143	572	157	380	603	1,196	735
	657	920	1,209	680	599	869	366
	159	1,053	982	1,251	160	1,152	711
	524						
rno-miR-30c	4,399	3,186	2,048	1,743	3,460	3,129	2,967
	4,042	3,566	2,348	3,738	3,869	2,729	2,188
	5,389	4,068	4,445	2,717	4,365	3,459	3,069
	3,347	5,216	3,430	2,186	4,234	3,126	3,549
	4,338	5,388	3,632	2,979	4,672	4,056	2,816
	2,994						
rno-miR-451	278	1,588	884	711	768	1,311	275
	444	1,352	737	1,413	1,789	801	591
	636	1,128	1,346	1,207	834	995	407
	397	2,192	559	1,229	1,035	1,811	746
	299	1,378	1,455	3,133	613	1,757	379
	749						

Supplement Table III. Absolute levels of miR-17/92 cluster

miR-17/92 cluster

	CTR	H day 2	H day 7	H day 21	M day 2	M day 7	M day 21
rno-miR-17	180	234	161	130	217	249	225
	184	164	338	201	260	246	272
	197	169	227	155	160	194	278
	214	323	352	184	158	314	175
	169	308	202	232	172	242	218
	250						
rno-miR-18a	29	21	28	16	8	28	23
	23	13	23	28	20	37	41
	16	26	30	25	25	21	30
	19	35	32	40	30	30	21
	22	31	25	24	18	16	40
	28						
rno-miR-19a	12	11	15	7	9	27	12
	12	33	17	12	11	16	17
	10	8	9	23	16	16	12
	9	39	14	21	17	10	14
	13	13	14	11	15	8	23
	16						
rno-miR-20a	268	272	241	216	239	284	264
	236	175	235	219	272	233	353
	214	257	263	300	238	267	281
	276	271	277	210	220	247	212
	216	302	316	108	225	252	248
	259						
rno-miR-19b	94	109	156	118	138	203	44
	83	144	90	199	194	80	113
	80	132	73	161	170	218	67
	39	479	51	102	166	79	141
	56	251	181	121	109	158	76
	100						
rno-miR-92a	418	487	519	500	490	438	509
	573	371	1,294	401	391	390	268
	922	524	708	380	454	415	392
	531	337	599	372	413	316	451
	553	507	453	249	670	444	553
	405						

Supplement Table IV: Predicted targets for the three downregulated miRNAs miR-21, miR-22 and miR-30c

Target name	Target of	Target function
KCNJ6	miR-22 and miR-30c	potassium inwardly-rectifying channel, subfamily J, member 6
PPP2R5E	miR-21 and miR-22	protein phosphatase 2, regulatory subunit B(B56), epsilon isoform
NFAT5	miR-22 and miR-30c	nuclear factor of activated T-cells 5
TACC1	miR-21 and miR-30c	transforming, acidic coiled-coil containing protein 1
ADARB1	miR-22	adenosine deaminase, RNA-specific, B1
TGFBR1	miR-22	transforming growth factor, beta receptor 1
TGFBRAP1	miR-22	transforming growth factor, beta receptor associated protein 1
RBPSUH	miR-21	recombining binding protein suppressor of hairless (Drosophila)
TNRC6A	miR-30c	trinucleotide repeat containing 6a
YWHAZ	miR-30c	tyrosine 3-monooxygenase/tryptophan 5-monooxygenase activation protein, zeta polypeptide

Supplement Table V. Predicted targets for the two up-regulated miRNAs miR-451 and miR-322

Target name	Also target of	Target function
ANKFY1		ankyrin repeat and FYVE domain containing 1
ANKS1A		ankyrin repeat and sterile alpha motif domain containing 1A
BCL9		B-cell CLL/lymphoma 9
CYBRD1		cytochrome b reductase 1
DHX37		DEAH (Asp-Glu-Ala-His) box polypeptide 37
DISP2		dispatched homolog 2 (Drosophila)
ELK4		ELK4, ETS-domain protein (SRF accessory protein 1)
FBXO21		F-box protein 21
GLS		glutaminase
GRM2		glutamate receptor, metabotropic 2
KCNJ6	**Mir-22 and miR-30c**	**potassium inwardly-rectifying channel, subfamily J, member 6**
KCNK5		potassium channel, subfamily K, member 5
KIAA0174		KIAA0174
MGAT4B		mannosyl (alpha-1,3-)-glycoprotein beta-1,4-N-acetylglucosaminyltransferase, isozyme B
MOBKL1B		MOB1, Mps One Binder kinase activator-like 1B (yeast)
NFAT5	**Mir-22 and miR-30c**	**nuclear factor of activated T-cells 5, tonicity-responsive**
PATL1		protein associated with topoisomerase II homolog 1 (yeast)
PDZD8		PDZ domain containing 8
PLXNC1		plexin C1
PMEPA1		prostate transmembrane protein, androgen induced 1
PPM1L		protein phosphatase 1 (formerly 2C)-like
RAB22A	**Mir-22 and miR-30c**	**RAB22A, member RAS oncogene family**
RCAN2		regulator of calcineurin 2
RGD1561661		similar to Ferritin light chain (Ferritin L subunit)
SAR1A		SAR1 homolog A (S. cerevisiae)
SLC11A2		solute carrier family 11 (proton-coupled divalent metal ion transporters), member 2
SLC12A2		solute carrier family 12 (sodium/potassium/chloride transporters), member 2
SLC25A22		solute carrier family 25 (mitochondrial carrier: glutamate), member 22
SNX11		sorting nexin 11
SNX27		sorting nexin family member 27
TACC1	**Mir-21 and miR-30c**	**transforming, acidic coiled-coil containing protein 1**
TGFA		transforming growth factor, alpha
TPCN1		two pore segment channel 1
UBE2K	**Mir-21 and miR-22**	**ubiquitin-conjugating enzyme E2K (UBC1 homolog, yeast)**
UBE4A		ubiquitination factor E4A (UFD2 homolog, yeast)
UNC5C		unc-5 homolog C (C. elegans)
ZBTB39		zinc finger and BTB domain containing 39
ZNF592		zinc finger protein 592